

國立交通大學

機械工程學系

碩士論文

利用廢熱回收提升進氣溫度對沼氣發電的影響研究

The Experimental Study on Biogas Power
Generation Enhanced by Using Waste Heat to Preheat
Inlet Gases



研究生：黃聖容

指導教授：陳俊勳 教授

中華民國一〇〇年六月

利用廢熱回收提升進氣溫度對沼氣發電的影響研究

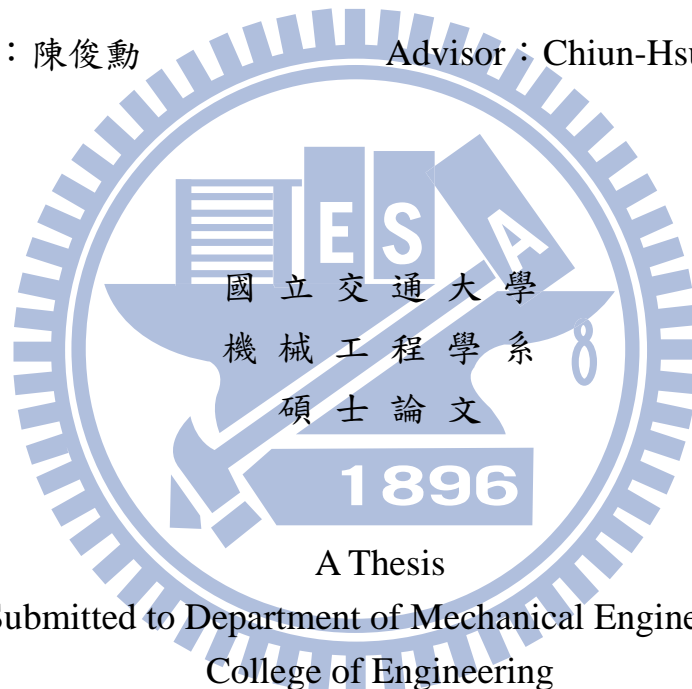
The Experimental Study on Biogas Power Generation Enhanced by Using
Waste Heat to Preheat Inlet Gases

研究生：黃聖容

Student: Sheng-Rung Huang

指導教授：陳俊勳

Advisor: Chiun-Hsun Chen



A Thesis

Submitted to Department of Mechanical Engineering
College of Engineering

National Chiao Tung University

In Partial Fulfillment of the Requirements

For the Degree of

Master of Science

In Mechanical Engineering

June 2011

Hsinchu, Taiwan, Republic of China

中華民國一〇〇年六月

利用廢熱回收提升進氣溫度對沼氣發電的影響研究

學生：黃聖容

指導教授：陳俊勳

國立交通大學機械工程學系

摘要

本論文在台中台糖養豬場測試小型 30kW 沼氣發電機，收集資料以供長時間沼氣發電使用。本論文分為三大部分，第一部分，使用 73% 甲烷濃度的沼氣，測試在不同沼氣供給量與不同過剩空氣比時的發電狀況；第二部分，將此結果與計畫第一年的 60% 甲烷濃度實驗數據比較，觀察不同甲烷濃度(60%與 73%)對發電效能之影響。第三部分，利用廢熱回收系統加熱進氣，測試不同進氣溫度對沼氣發電的影響。實驗結果顯示，使用目前 73% 之甲烷濃度沼氣，在沼氣供給量為 260L/min 時，引擎最佳發電量為 26.7kW；在沼氣供給量為 200L/min 時擁有最佳熱效率 27% 和最佳甲烷使用率 96.03%。提升甲烷濃度，發電功率隨著甲烷濃度提升而提升，除了當過剩空氣比 $\lambda < 0.85$ 時。對熱效能而言，在燃料量較稀的狀況下 ($\lambda > 0.95$) 可讓熱效能提升；但在燃料量較濃的狀況下 ($\lambda < 0.95$)，提升甲烷濃度對熱效能沒有好的影響。提升進氣溫度，在過剩空氣比約大於 1.3 後有較明顯的影響。

關鍵字: 沼氣、沼氣發電、沼氣濃度、進氣溫度

The Experimental Study on Biogas Power Generation Enhanced by Using Waste Heat to Preheat Inlet Gases

Student: Sheng-Rung Huang

Advisor: Prof. Chiun-Hsun Chen

Department of Mechanical Engineering
National Chiao Tung University

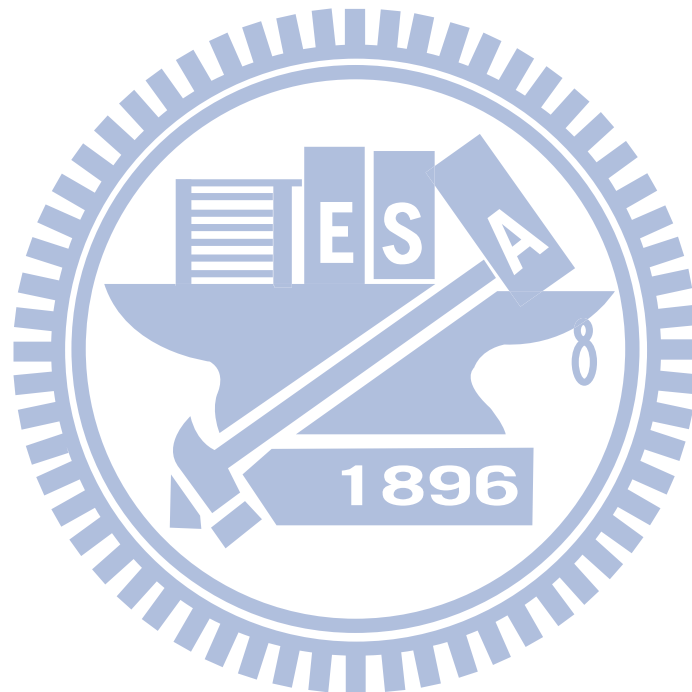
ABSTRACT

This research used a 30kW-generator in Taiwan Sugar swine farm in Taichung to collect data for the long-term electricity generation. This study is an continuous effort of Lin's work [3], which carried out the electricity generation project by using 60% methane concentration of biogas in a small swine farm in Miaoli. This experimental study, using 73% methane concentration of biogas, consisted of three parts. Firstly, investigate the effect of biogas supply rate together with the different excess air ratios on generator performance. Secondly, make a comparison with Lin's results. Finally, apply a waste heat recovery system to preheat the inlet gas under different temperatures and analyze the preheating influence on the generator performance.

In the present study, the maximum power generation is 26.7kW occurred at biogas flow rate of 260L/min, whereas the maximum thermal efficiency and methane consumption ratio are 27% and 96.03% at biogas flow rate of 200L/min. The power generation in the present work is higher than one in Lin's one [3], except the region around λ (excess air ratio) < 0.85 . However,

the thermal efficiency increases with the increasing methane concentration just in the region of $\lambda > 0.95$, while on the relatively rich side ($\lambda < 0.95$), there is no benefit. The improvement by preheating inlet gas is obvious when excess air ratio is relatively high, such as $\lambda > 1.3$.

Keywords: Biogas, Biogas generator, Methane concentration, Inlet gas temperature



Acknowledgements

首先要感謝指導教授 陳俊勳老師，您嚴謹的教學方式，使我在研究生涯中獲益良多，不僅只於學問上的研究，還有為自己負責的態度。並感謝國科會計畫的經費支持，讓我的實驗能夠持續下去。

感謝宗翰學長的指導，讓我了解實驗的方法和計畫報告的處理方式，使我的研究之路變得順遂。並感謝實驗室其它學長阿貴、昶安、金輝、家維、塘原，在生活和學習中適時給我協助與建議。謝謝你們！

感謝同學云婷、抓抓、世庸、黃鈞你們的陪伴，讓我在這條路上不孤單。謝謝學弟們平日的搞笑，舒緩我的壓力，小豬、天洋、阿扁、鈺鈞，謝謝你們。

最後，謹以此文獻給我的雙親。



Contents

ABSTRACT(Chinese)	i
ABSTRACT(English)	ii
Acknowledgements	iv
Contents	v
LIST OF TABLE	viii
LIST OF FIGURES	x
Chapter 1	1
Introduction	1
1.1 Motivation and Background:	1
1.2 Literature Review	5
1.3 Scope of Present Study	14
Chapter 2	16
Biogas System in Swine Farm	16
2.1 Swine Manure Management	16
2.2 Three-step Piggery Wastewater Treatment (TPWT)	16
2.2.1 Solid-liquid Separation	17
2.2.2 Anaerobic Treatment	17
2.2.3 Aerobic Treatment	18
2.3 Utilization of Biogas	19
2.4 Engines	21
2.4.1 Four-stroke Gas Engine and Diesel Engine	21
2.4.2 Stirling Engine	22

2.4.3 Gas Turbine.....	22
2.4.4 Micro Gas Turbine.....	23
2.4.5 Fuel Cell.....	23
Chapter 3	25
Experimental Apparatus and Procedures	25
3.1 Experiment layout	25
3.1.1 Engine	25
3.1.2 Air Flow Meter (VA-400).....	26
3.1.3 Biogas Flow Meter (TF-4000).....	27
3.1.4 Thermocouple	27
3.1.5 Gas Analyzer (HM5000)	28
3.1.6 Methane Concentration Analyzer	28
3.1.7 Heat Exchanger.....	28
3.1.8 Data Acquisition	28
3.1.9 Temperature Monitor.....	29
3.1.10 Humidity Temperature Meter (Center 311).....	29
3.2 The Theoretical Calculation.....	30
3.3 The Effect of Methane Concentration.....	33
3.4 The Effect of Intake Gases Temperature	34
Chapter 4	36
Results and Discussion.....	36
4.1 Effect of Excess Air Ratio (λ).....	36

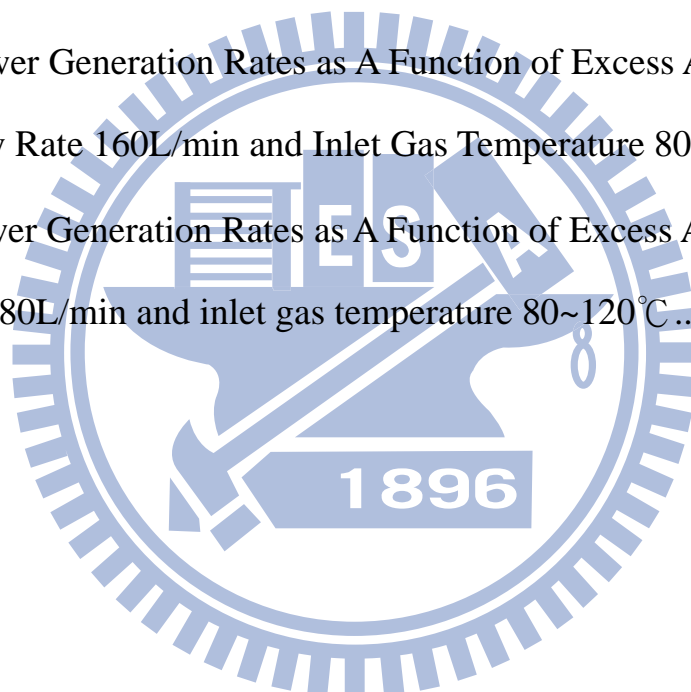
4.2 Effect of Methane Concentration.....	46
4.3 Effect of Inlet Gas Temperature	51
4.4 Comparison with Other Researches.....	55
Chapter 5	57
Conclusions and Recommendations	57
5.1 Conclusions.....	57
References	59



LIST OF TABLE

Table 1.1 Biogas contents from different biogas producing plants [2]	2
Table 3.1 Engine Technical Data.....	26
Table 3.2 Specifications of the data acquisition modules	29
Table 4.1 Limiting value of air supply for each biogas supply rate	37
Table 4.2a Power Generation Rates as A Function of Excess Air Ratio at Biogas Volume Flow rate 140L/min	42
Table 4.2b Power Generation Rates as A Function of Excess Air Ratio at Biogas Volume Flow rate 160L/min	42
Table 4.2c Power Generation Rates as A Function of Excess Air Ratio at Biogas Volume Flow rate 180L/min	43
Table 4.2d Power Generation Rates as A Function of Excess Air Ratio at Biogas Volume Flow rate 200L/min	43
Table 4.2e Power Generation Rates as A Function of Excess Air Ratio at Biogas Volume Flow rate 220L/min	44
Table 4.2f Power Generation Rates as A Function of Excess Air Ratio at Biogas Volume Flow rate 240L/min	44
Table 4.2g Power Generation Rates as A Function of Excess Air Ratio at Biogas Volume Flow rate 260L/min	45
Table 4.3 The Maximum Excess Air Ratio of Biogas Flow Rate with 60% and 73% CH ₄ of Biogas.....	47
Table 4.4a Power Generation Rates as A Function of Excess Air Ratio at Biogas Volume Flow rate 180L/min with 60% CH ₄ [3].....	50
Table 4.4b Power Generation Rates as A Function of Excess Air Ratio at Biogas Volume Flow rate 200L/min with 60% CH ₄ [3].....	50

Table 4.4c Power Generation Rates as A Function of Excess Air Ratio at Biogas Volume Flow rate 220L/min with 60% CH ₄ [3].....	50
Table 4.4d Power Generation Rates as A Function of Excess Air Ratio at Biogas Volume Flow rate 240L/min with 60% CH ₄ [3].....	51
Table 4.4e Power Generation Rates as A Function of Excess Air Ratio at Biogas Volume Flow rate 260L/min with 60% CH ₄ [3].....	51
Table 4.5a Power Generation Rates as A Function of Excess Air Ratio at Biogas Supply Rate 140L/min and Inlet Gas Temperature 80~120°C	54
Table 4.5b Power Generation Rates as A Function of Excess Air Ratio at Biogas Supply Rate 160L/min and Inlet Gas Temperature 80~120°C	54
Table 4.5c Power Generation Rates as A Function of Excess Air Ratio at Biogas Supply Rate 180L/min and inlet gas temperature 80~120°C	55



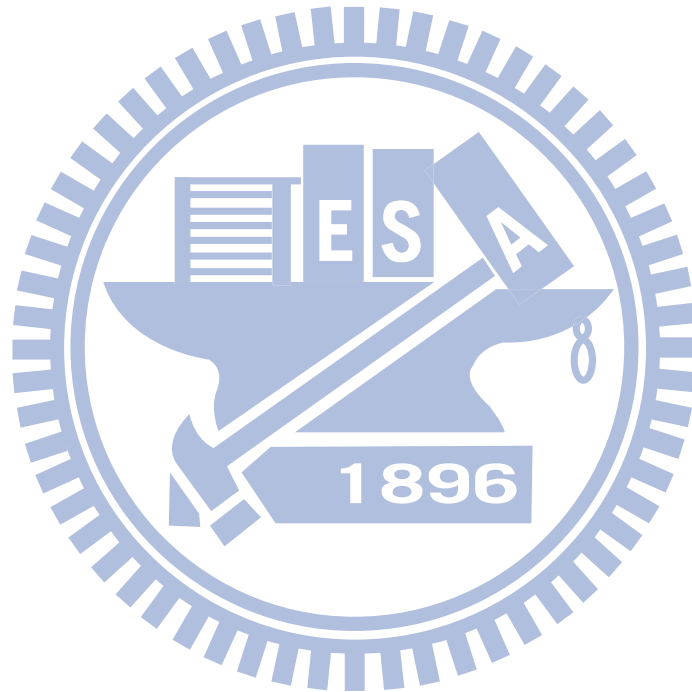
LIST OF FIGURES

Fig. 1.1 Carbon dioxide emissions avoided via the use of renewable energy sources in Germany 2009. [26]	63
Fig. 1.2 Simple Carbon Cycle for Biogas [3]	63
Fig. 1.3 Scope of this Research	64
Fig. 2.1 Range of Capacities for the Power Generators.....	65
Fig. 2.2 Values of Power Generators.....	65
Fig. 3.1a Experiment Layout.....	66
Fig. 3.1b Waste Heat Recovery Layout.....	66
Fig. 3.2 Four stroke diesel engine	67
Fig. 3.3a VA-400 flow sensor	68
Fig. 3.3b VA-400 flow sensor data	68
Fig. 3.4a TF-4000 Flow meter	69
Fig. 3.4b TF-4000 Flow Meter Data	70
Fig. 3.5 K-Type Thermocouple.....	71
Fig. 3.6 HM5000Gas Analyzer	71
Fig.3.7 Guardian Plus Infra-Red Gas Monitor.....	72
Fig 3.8 Heat Exchanger	72
Fig. 3.9a CompactDAQ Chassis	73
Fig. 3.9b NI 9203 Analog Input Module.....	73
Fig. 3.9c NI 9211 Analog Input Module	74
Fig.3.10 Temperature Monitor	74
Fig.3.11 Center 311 Humidity Temperature Meter	75
Fig. 4.1 Power generation v.s. excess air ratio at different biogas supply rates	76

Fig. 4.2 Thermal efficiency v.s. excess air ratio at different biogas supply rates	76
Fig. 4.3 Waste gas temperature v.s. excess air ratio with different biogas supply rates	77
Fig. 4.4 O ₂ concentration in waste gas v.s. excess air ratio with different biogas supply rates.....	77
Fig. 4.5 CO ₂ concentration in waste gas v.s. excess air ratio with different biogas supply rates	78
Fig. 4.6 NO _x concentration in waste gas v.s. excess air ratio with different biogas supply rates	78
Fig. 4.7 Estimated CH ₄ consumption ratios in combustion v.s. excess air ratio with different biogas supply rates	79
Fig. 4.8 Power generation with different methane concentrations of biogas	79
Fig. 4.9 Thermal efficiency with different methane concentrations of biogas	80
Fig. 4.10 Waste gas temperature with different methane concentrations of biogas.....	80
Fig. 4.11 Power generation of biogas supply rate 180 L/min v.s. excess air ratio with different inlet gas temperatures.....	81
Fig. 4.12 Thermal efficiency of biogas supply rate 180 L/min v.s. excess air ratio with different inlet gas temperatures	81
Fig. 4.13 Power generation of biogas supply rate 160 L/min v.s. excess air ratio with different inlet gas temperatures	82
Fig. 4.14 Thermal efficiency of biogas supply rate 160 L/min v.s. excess air ratio with different inlet gas temperatures	82

Fig. 4.15 Power generation of biogas supply rate 140 L/min v.s. excess air ratio with different inlet gas temperatures 83

Fig. 4.16 Thermal efficiency of biogas supply rate 140 L/min v.s. excess air ratio with different inlet gas temperatures 83



Chapter 1

Introduction

1.1 Motivation and Background:

Global warming and energy shortage crisis are serious problems for human beings now. Therefore, controlling the emissions of greenhouse gases and finding alternative energy become international issues.

Recently, people pay a lot of attention to renewable energy, including hydropower, solar thermal energy, wind energy, geothermal energy and biomass energy. Renewable energy, which has a great potential substitution of fossil fuel, is an important part of carbon offset, it not only can avoid the carbon dioxide produced from the fossil fuel (see Fig. 1.1), but also has renewability to handle energy shortage crisis.

Biomass energy, a kind of renewable energy, becomes more popular due to its contribution to energy supply and environmental protection in the same time. It comprises about two thirds of total renewable energy. The source of biomass energy can be derived from plant or animal organic matter, such as waste, wood, gas, etc.

Biogas is one of the biomass energy resources, it can be generated from many places, including landfill, farm biogas plant and sewage digester. Different sources of biogas contain different components, which is illustrated in Table 1.1. Concerning with the reduction of carbon dioxide emission and high dependence on import energy, which was 98.2% in 1998, 99.0% in 2003, and 99.3% in 2008 [1], in Taiwan, biogas appears to be an attractive energy resource.

Table 1.1 Biogas Contents from Different Biogas Producing Plants [2]

Biogas	CH ₄ (%)	CO ₂ (%)	O ₂ (%)	N ₂ (%)	H ₂ S (ppm)	Benzene (mg m ⁻³)	Toluene (mg m ⁻³)	Ref.
Landfill	47–57	37–41	<1	<1–17	36–115	0.6–2.3	1.7–5.1	^a
Sewage digester	61–65	36–38	<1	<2	b.d.	0.1–0.3	2.8–11.8	^a
Farm biogas plant	55–58	37–38	<1	<1–2	32–169	0.7–1.3	0.2–0.7	^a
Landfill	59.4–67.9	29.9–38.6	n.a.	n.a.	15.1–427.5	21.7–35.6	83.3–171.6	[7]
Landfill	37–62	24–29	<1	n.a.	n.a.	<0.1–7	10–287	[4]
Landfill	55.6	37.14	0.99	n.a.	n.a.	3.0	55.7	[6]
Landfill	44	40.1	2.6	13.2	250	n.a.	65.9	[8]
Sewage digester	57.8	38.6	0	3.7	62.9	n.a.	n.a.	[21]
Sewage digester	62.6	37.4	n.a.	n.a.	n.a.	n.a.	n.a.	[22]
Sewage digester	58	33.9	0	8.1	24.1	n.a.	n.a.	[23]

b.d.—Below detection limit 0.1 ppm. n.a.—not analysed.

^aThis study.

Animal manure of the farm can produce biogas after anaerobic treatment. The main components of the biogas are methane (CH₄) and carbon dioxide (CO₂) with relatively little amounts of nitrogen (N₂), hydrogen (H₂), ammonia (NH₃), hydrogen sulfide (H₂S) and organic compounds. Methane inside the biogas is a flammable fuel, therefore, such biogas can be used as renewable fuel, provided that methane content is sufficient enough.

The main greenhouse gases in atmosphere are water vapor, carbon dioxide, methane, nitrous oxide, ozone and chlorofluorocarbons. When the earth is radiated by the sun light, part of radiation is reflected to the outer space, another part of radiation is absorbed by the earth's surface. These greenhouse gases can absorb the heat energy emitted by the earth surface, leading to the increasing temperature of atmosphere. There are many benefits using the farm biogas. First of all, untreated manure contains nitrous oxide (NO_x), carbon dioxide (CO₂) and methane (CH₄) gases. The greenhouse potential of methane is 23 times of the carbon dioxide. If those gases emit into the surroundings, the impact to the environment is huge. Furthermore, the biogas is a carbon neutral energy resource. Unlike fossil fuels that releases carbon dioxide which is captured by billion years ago, carbon dioxide released by the biogas which is captured recently. The carbon in the biogas comes from the photosynthesis through plants, and after burning it, the carbon dioxide goes back to the

surroundings, so the net of carbon amount in this cycle is zero (see Fig. 1.2 for the illustration). However, the carbon of fossil fuels is out of the carbon cycle because they are captured long time ago, and its combustion leads more carbon dioxide content in environment. For this reason, biogas can make balance of greenhouse gas emissions in earth. In other words, biogas is an environmentally friendly fuel. Second, animal manure has lots of organic matters, which lead the river quality to become deteriorated, and wastewater treatment can avoid the further pollution. Third, biogas can generate power that has great potential to reduce the amount of import energy by this way in Taiwan. Last, biogas is a renewable energy resource. The carbon of the biogas comes from photosynthesis through plants. As long as the sun continues emitting light, the energy supply will not stop. Beside, according to the survey of Tsai and Lin [4], with a practical basis of the total swine population from the farm scale of over 1000 heads, the usage of bio-energy from swine manure management showed following benefits: emissions of methane reduce 21.5 Gg, total electricity is generated of 7.2×10^7 kW-h per year, equivalent to electricity charge saving of USD 7.2×10^6 , and carbon dioxide mitigation is of 500 Gg per year. To sum up, biogas is a renewable and green alternative energy fuel.

This laboratory has been awarded a three-year research project by National Science and Technology Program for Energy from 2010 to 2012. The project is named as *Development the technology of agricultural waste bioconversion to biogas for electricity generation and carbon dioxide elimination by microalgae*. Constructing a pilot biogas plant is the ultimate goal of this project. The project is divided into four subprojects. The subproject 1 is to upgrade the utilization efficiency of biogas by removing H₂S and CO₂ to improve the biogas generation rate. In the subproject 2, the desulfurized biogas of subproject 1 will

be utilized to operate the biogas engine to produce electricity under different monitoring parameters. The subproject 3 is to produce biodiesel from high lipid-content algae utilizing waste CO₂ either from the engine flue gas or the biogas itself. The purpose of subproject 4 is to research the operating conditions which will affect biogas production rates and methane concentrations emission during the anaerobic processes.

This study is originated from the subproject 2 mentioned above. In the first year, the subproject uses a 30kW generator as a vehicle to build a waste heat recovery system and to analyze the power supply and efficiency for the system in a small scale. In the second year, based on the achievements and experience from the first year, a pilot plant is constructed for biogas and power plant in Taiwan Sugar swine farm. In the meantime, a fuzzy control system is also installed to enhance the performance. In the third year, a completely self-operated biogas plant with CHP system is constructed. By 2010, this subproject is capable to generate 90,000kW-h electricity per year, equivalent to electricity charge saving of 270 thousand NT dollars, in an order of 2000 pigs.

In the first year, Lin [3] tested different air-fuel ratio for 30kW generator with 60% methane concentration of biogas in a small swine farm in Miaoli. The oxygen-enriched combustion and heat recovery were also applied to his research. The results showed that the efficiency of the generator is improved by using oxygen-enriched combustion and heat recovery system. For the following years, the biogas plant is enlarged in Taiwan Sugar swine farm in Taichung. This study mainly will test the scale-up effect based on Lin's research [3].

1.2 Literature Review

Chen et al. [1] analyzed renewable energy situation in Taiwan, such as biomass energy, solar energy, wind power, geothermal energy and hydropower etc. They indicated that renewable energy has not yet fully developed in Taiwan because the fossil energy is cheaper than renewable one. However, the renewable energy will become more competitive in the energy market since Legislative Yuan passed “Renewable Energy Development Bill” in June 2009. Besides, the promotion of the renewable energy will offer positive economic benefits for the related industry.

Rasi et al. [2] researched biogas component and variation in landfill, sewage treatment plant sludge digester, and farm biogas plant to analyze its potential used as bio-energy. They found that the biogas compounds vary with different biogas plants: carbon dioxide ranges from 36% to 41%, methane from 48% to 65%, nitrogen from 1% to 17% and oxygen content is less than 1%. Sewage digester biogas contains highest methane content, landfill biogas contains lowest methane and highest nitrogen contents in winter. The total volatile organic compounds (TVOCs) range from 5 to 268 mg/m³, and the farm biogas plant has the lowest TOVCs. The sulphur compounds are found in all three places.

Lin [3] tested different air-fuel ratios for 30kW generator with 60% methane concentration of biogas in a small swine farm in Miaoli. The oxygen-enriched combustion and heat recovery were also applied to his research. The results showed that a higher power output and better thermal efficiency can be achieved by a greater conversion of CH₄ in the combustion process. The engine performances are not improved much by 1% oxygen-enriched air, but

with 3% oxygen-enriched air, the maximum power generation and thermal efficiency are increased, especially the engine now can be operated normally at a lower limiting fuel supply rate. The heat recovery system is used to heat water, leading to an improvement of overall efficiency.

Tsai and Lin [4] surveyed bio-energy from livestock manure management in Taiwan. With a practical basis of the total swine population from the farm scale of over 1000 heads, the analysis showed following benefits: emissions of methane reduce 21.5 Gg, total electricity is generated of 7.2×10^7 kW-h per year, equivalent to electricity charge saving of USD 7.2×10^6 , and carbon dioxide mitigation is of 500 Gg per year.

Su et al. [5] established greenhouse gas production data from anaerobic livestock wastewater treatment processes in Taiwan, and made the difference between the livestock wastewater treatment system in Taiwan and that presented by the IPCC. The data revealed that anaerobic wastewater treatment systems of pig and dairy farms emit 0.768 and 4.898 kg CH₄, 0.714 and 4.200 kg CO₂, and 0.002 and 0.011 kg N₂O per year per head during three temperature periods. Because animal manure is diluted before being treated with a solid/liquid separator and an anaerobic wastewater treatment system, the average emissions rates of CH₄ in the selected pig and dairy farms are lower than the limits imposed by the IPCC.

Yang et al. [6] estimated of methane and nitrous oxide emissions from animal production sector in Taiwan during 1990~2000. Methane emission from enteric fermentation of livestock was 30.9 Gg in 1990, increased to 39.3 Gg in 1996, and decreased to 34.9 Gg in 2000. Methane emission from the waste management was 48.5 Gg in 1990, 60.7 Gg in 1996, and 43.3 Gg in 2000. In the case of poultry, methane emission from enteric fermentation and waste

management were 30.6~44.1 ton and 8.7~13.2 Gg. Nitrous oxide emission from waste management of livestock was 0.78 ton in 1990, 0.86 ton in 1996, and 0.65 ton in 2000. Nitrous oxide emission from waste management of poultry was higher than that of livestock with 1.11 ton in 1990, 1.68 ton in 1999, and 1.65 ton in 2000.

Saiful Bari [7] used carbon dioxide and nature gas, which contained about 96% methane, to simulate the operation of diesel engine in dual-fuel mode with biogas containing various percentages of carbon dioxide. They found out when biogas contains more than 40% carbon dioxide, the engine runs harshly. The trend of bsfc (brake specific fuel consumption) curve decreases in 20 to 30 per cent carbon dioxide region, but raises beyond certain (20 to 30) per cent of carbon dioxide region. It is because the carbon dioxide can be dissociated into carbon monoxide and oxygen under high temperature, and the carbon monoxide is comparatively fast burning gas than other alternative fuels, in the meantime, the oxygen from the dissociation increases the concentration of oxygen in the gas air mixture, leading to reducing the ignition delay and enhancing the combustion of unburned carbon particles. But when the carbon dioxide content is beyond certain region, the carbon dioxide becomes higher for the superfluous carbon dioxide remains undissociated, making the curve of bsfc to rise with an increase carbon dioxide concentration.

Duc et al. [8] used a small IDI biogas premixed charge diesel dual fuelled CI engine to test Diesel fuel substitution, engine performance, energy consumption and long term operation. They obtained following results. First, although the diesel dual fuel (DDF) mode has lower energy conversion efficiency, it can be offset by the reduced fuel cost of biogas over diesel. At low and medium loads, the DDF engine produces higher UHC (unburnt hydrocarbon) and less soot,

leading to a reduction in efficiency. When engine load increases to full load the conversion efficiency is good as that in diesel fuelling. Second, the engine operates in DDF mode has the lower exhaust gas, higher lube oil and higher cooling water temperatures than those temperatures in diesel mode. Last, as a gas mixer is installed, the temperatures of oil and cooling water increases and lube oil sucks to the cylinder, resulting in high lube oil consumption. So, the engine cannot withstand the higher thermal load under DDF mode at the engine speeds and loads proposed for diesel fuel.

Tippayawong et al. [9] used biogas and diesel mixed fuel to feed a small diesel engine and examined its endurance over 2000 hours. The results showed that engine has 7% of higher power output and higher efficiency compared to that in normal diesel operation.

Alasfour [10] used 30% iso-butanol-gasoline blend and preheated the inlet air to investigate the NO_x emission in a spark ignition engine. The results showed that the maximum level of NO_x emission is reduced by 9% in 30% iso-butanol-gasoline blend comparing to gasoline. When the inlet air temperature increases from 40 to 60°C, the NO_x emission will increase 10% at a fuel/air equivalence ratio of 0.9.

Porpatham et al. [11] tested the effect of CO_2 concentration in biogas on the performance of constant speed spark ignition (SI) engine. A lime water scrubber was used to absorb carbon dioxide (CO_2) in biogas. They found when carbon dioxide (CO_2) in biogas is reduced from 41% to 30%, then 20% of engine performance is improved, unburned hydrocarbons (HC) is reduced and lean limit of combustion is extended. However, such improvement occurs just in the lean-fuel region. Increasing methane concentration plays a significant role in lean-fuel region because the flame velocities are low in such region. There is

no benefit for power and efficiency on the rich-fuel side due to incomplete combustion of engine.

Borjesson and Berglund [12] analyzed the emissions of nitrogen oxides (NO_x), carbon dioxide (CO_2), carbon oxide (CO), sulphur dioxide (SO_2), hydrocarbons (HC), methane (CH_4), and particles from a life-cycle for different biogas systems on six different raw materials. They identified that the biogas systems emit lots of gases mentioned above, and the emissions are affected by the properties of the raw material digested, the energy efficiency of the biogas production, and the end-use technology. Between two biogas systems that provide an equivalent energy service, fuel-cycle emission may vary by a factor of 3–4, and for certain gases the factor by up to 11. There are extensively significant source of emissions, for example, waste-products or ley cropping.

Abd-Alla et al. [13] operated a high speed indirect injection dual fuel engine, using methane and sometimes propane as main fuel and Diesel fuel as pilot fuel. The effects of exhaust gas recirculation (EGR), diluents admission (N_2 and CO_2), and intake air temperature on combustion and emissions were concerned. The results showed that the admission of diluents reduce the NO_x emissions, the higher intake temperature increases the NO_x emissions but reduces the unburned hydrocarbon emission.

Tsagarakis [14] analyzed optimal number of energy generators for biogas utilization in wastewater treatment facility. The data of this analysis was based on the first generator for energy production from biogas, and it had been operated for 5.5 years. If one generator is used, the cost per kWh produced is 0.0876 €/kWh covering 15.9% of the facility's needs. If two generators are used, the average cost for energy production is 0.0881€/kWh covering 32.6% of the facility's needs. The estimations of six generators have been made. The

economic analysis is calculated by total annual economic cost, which is the sum of the annuitized construction cost and the annual operation and maintenance costs. The results showed that the cost of each kWh produced may increase when the number of generators is increased, the cost decreases when the lifetime of generator increases.

Semin et al. [15] compared the cylinder pressure and maximum pressure of the compressed natural gas engine with original diesel engine. The result showed that the transform of diesel engine into compressed natural gas engine decreases the cylinder pressure.

Torregrosa et al. [16] tested the effect of coolant and inlet charge temperature on the emission reduction and performance of DI Diesel engines. The coolant temperature ranged from 65 to 97°C. The intake charge temperature ranged from 44 to 68 °C. The results show that the coolant temperature has low effects on engine operation. There is no effect at medium or higher load. The NO_x emissions decrease and HC emissions increase for lower wall temperature at low loads. Intake air temperature influences NO_x formation for all the loads, as the temperature increases the NO_x emissions increase. But its influence on HC emissions is restricted to low loads, as the temperature increases the HC emissions decrease. For engine, HC emissions are the result of incomplete combustion, and the higher HC emissions imply the lower fuel conversion efficiency.

Zarante et al. [17] operated four-cylinder, flexible fuel engine, using gasoline and nature gas as fuels, to evaluate the exhaust emissions of carbon monoxide (CO) and carbon dioxide (CO₂). Due to the low carbon-hydrogen ratio of nature gas with regard to gasoline, the CO₂ emission of nature gas is less than that of gasoline. Also the CO emission of nature gas is less than that of gasoline,

because the engine can operate with leaner mixtures when natural gas is used instead of gasoline.

Ga et al. [18] used biogas-gasoline hybrid engine to test the conversion efficiency of the biogas. The results showed that 1 m³ of biogas can produce 1kW-h electricity and reduce 1kg CO₂ emission in the atmosphere.

Cho et al. [19] made a review for spark ignition of natural gas engines. In order to meet the emission standards and consider the stable combustion of engine, several methods can be used. First, lean burn is an effective way to reduce NO_x emissions, but for recovering power output losses, turbocharging technology should be considered. Second, stoichiometric natural gas engine can equip with three-way catalyst to convert CO, HC and NO_x, however, air-fuel ratio controller is needed. Third, EGR can improve knocking situation by reducing combustion temperature.

Huang and Crookes [20] diluted natural gas by using CO₂ to simulate biogas as fuel in single-cylinder spark-ignition engine. The fraction of CO₂ in simulated biogas was ranged from 0 to about 40%. They tested the effects of CO₂ fraction, relative air-fuel ratio, engine speed and compression ratio on the engine performance and exhaust gas emissions. The measured results included power, thermal efficiency, exhaust temperature and mole fractions of the emissions CO, NO_x and unburnt hydro-carbon in exhaust gases. The following are conclusions obtained from experimental results: First, increasing the fraction of CO₂ in biogas can lower the NO_x emission and enable the compression ratio to be increased. However, it would reduce cylinder pressure that results in the reductions of power and thermal efficiency, and the increases of unburnt hydrocarbon emissions at the same time. Second, the CO emissions are low and change little when running with fuel-lean mixture. As running

with fuel-rich mixture, the CO emissions increase sharply when CO₂ fraction is above 30% due to incomplete combustion. The CO emissions are almost unaffected by compression ratio and engine speed. Third, when the compression ratio becomes higher, the brake mean effective pressure, brake efficiency and emissions of NO_x and unburnt hydrocarbon become higher. But when the compression ratio is above 13:1, the power and thermal efficiency increase slightly and the emissions of CO increase. As the compression ratio is further above 15:1, the detonations occur. Fourth, the highest power and thermal efficiency occur with compression ratio between 13:1 and 15:1 and the relative air-fuel ratio between 1.05 and 0.95. In this range, the emissions of CO and unburnt hydro-carbon are low but the NO_x emissions are relatively high.

Nathan et al. [21] converted a single-cylinder, diesel engine to operate in homogeneous charge compression ignition (HCCI) mode with acetylene as fuel. They tested the effects of intake air temperature and exhaust gas recirculation (EGR) on the engine performance and exhaust gas emissions. The intake air was heated by an electric heater in the range of 40~110°C from no load to brake mean effective pressure (BMEP) of 4 bar. The results showed that the intake air temperature and amount of EGR have to be controlled according to engine output. At high engine output, engine is very sensitive to the intake air temperature and EGR. In order to get greater brake thermal efficiency, precise control is required. It is observed that the best charge temperature is reduced as BMEP increases, because the elevation of BMEP will lead to an increase of engine temperature and make the mixture become richer. When the mixture is rich, the self-ignition temperature reduces and the combustion rate increases. Besides, at high BMEPs, using EGR will lead to knock.

Badr et al. [22] carried out a parametric study on the lean misfiring and knocking limits of gas-fueled spark ignition engine. They tested Ricardo E6 engine, using propane and liquefied petroleum gas (LPG) as fuels. The parameters included engine speed, compression ratio, spark timing, intake temperature, intake pressure, and relative humidity of intake air. The following are experimental results: Advancing the spark timing leads to the reduction of lean misfire and knocking limit. For low engine speeds, when the intake temperature increases, the lean misfire limit decreases. For high speeds, when the intake air temperature is up to 70°C the lean misfire limit increases, beyond 70°C the lean misfire decreases. As the relative humidity of the intake air increases, the lean misfire limit increases because the water vapors as a diluents will damp down the reaction rates during compression and combustion processes.

Sridhar et al. [23] revealed the misunderstanding when gas as a piston engine fuel. They converted multi-cylinder diesel engine into spark ignition engine, and the compression ratio ranged from 11.5:1 to 17:1. The results showed that the engine can run smoothly without auto-ignition tendency at high compression ratio (17:1). Besides, the engine can get higher efficiency and more brake power when working at higher compression ratio. However, comparing with diesel mode, the maximum de-rating in power is 16% and the overall efficiency drops down by almost 32.5% in gas mode. The analysis revealed that excess energy loses to coolant due to combustion chamber design. In order to improve the efficiency, the combustion chamber design for gas fuel is needed in the future.

Tricase and Lombardi [24] evaluated the development of biogas in Europe and Italy. The amount of biogas increases gradually, and the usage of biogas

depends on biogas quality. The percentage of biogas for generating electricity is 2/3 of total amount, and for generating heat is 1/3 nowadays. While Great Britain and Germany are the main producing countries so far, France has the highest production potential in the future. Most of Italian biogas is from landfills, and the biogas from animal waste is only small percentage of total.

Chung et al. [25] tested the chemical absorption and a biological oxidation process to remove high H_2S concentrations. The results suggested that the liquid flow rate in the biological oxidation reactor was controlled at 3 mL/min, the volume ratio of biological reactor to chemical reactor was 13.5:1 when 150 g-S/m³/h of inlet H_2S loading was introduced to the system.

1.3 Scope of Present Study

The scope of this research is presented in Figure 1.3. The goal of this research is to test a 30kW-generator in a swine farm.

The energy balance for overall biogas into the energy cycle is measured and calculated. The treatments of biogas include three-step piggery wastewater treatment system and H_2S removal system, and all of them need energy to operate. So the net energy output from biogas-powered generator should deduct to the energy consumption by the systems.

The methane concentration of biogas can be affected by the organics concentration in wastewater. The usage of water to clean and cool the pigpen changes the organics concentration in wastewater, leading to variation of methane (CH_4) concentration in biogas. So the first task of this study is to test the effects of different methane (CH_4) concentrations in biogas on the generator performance with different fuel flow rates and excess air ratios.

These results will compare with other corresponding experimental ones. Secondly, build waste heat recovery system to preheat inlet gases (the mixture of biogas and air) under different temperatures and analyzes the preheating influence on the generator performance.



Chapter 2

Biogas System in Swine Farm

2.1 Swine Manure Management

Swine production is very important in the agriculture of Taiwan. If the amount of wastewater produced by a pig is estimated as 20 liters per day, then the total wastewater produced by 6.6 million pigs (the total number of pigs in Taiwan) is 19 tons per day, making as the third most pollution source in Taiwan that is behind the sewage and industrial wastewater.

In 1987, the quality of waste water draining from livestock farms has to meet the governmental standards. Since then, a great variety of wastewater treatment technologies have been developed. Among them, the three-step waste treatment system developed by the Taiwan Livestock Research Institute (TLRI), which includes solid-liquid separation, anaerobic treatment and aerobic treatment (activated sludge treatment system), is regarded and accepted as one of the best systems in Taiwan, and has been extended to hog farms since 1987. Via the three-step treatment, both the Biochemical Oxygen Demand (BOD) and Suspended Solids (SS) of treated water can be less than 100 mg per liter.

2.2 Three-step Piggery Wastewater Treatment (TPWT)

The three-step piggery wastewater treatment system is based on a typical continuous plug-flow design, and the volume of raw wastewater remains constant over each 24-hour period. Under optimal operation conditions, wastewater thus flows into the system and is discharged continuously. Anaerobic treatment is conducted after solid/liquid separation, and occurs

inside of anaerobic basins covered with “red-mud plastic cover” (1.2~1.8mm of thickness), made of a kind of PVC material, which is corrosion-resistant and gas-and-water impermeable. Anaerobic treatment is generally slower than forced aeration, but consumes less energy. The anaerobic treatment system of TPWT process can also salvage a part of chemical energy content of wastewater by generating methane, a useful fuel. The optimal hydraulic retention time is around 4–6 days, and BOD removal is expected to be more than 80%.

2.2.1 Solid-liquid Separation

Separation of the solid fraction from the wastewater is to reduce the content of solids for subsequent handling and treatment, and to recover the solids for using as fertilizer, etc. This physical process is accomplished by using various kinds of filters. The efficiency of this treatment is a 15-30% decrease in BOD and a 50% decrease in SS. The moisture content of the separated solids is 70-80%. An extruder is often added to reduce the water content of the solids to 70% or below so that the material is suitable for composting.

2.2.2 Anaerobic Treatment

Since hog wastes are biodegradable, biological treatment is generally an economical way of handling them. The horizontal tent-type anaerobic fermenter is a modification of the Red Mud Plastic (RMP) bag fermenter which was also developed by the Taiwan Livestock Research Institute. Among its merits are the fact that it is easy to construct, has a low investment cost, is easy to maintain, and can be separated into several divisions as desired. These fermenters can be sealed from either inside or outside. The four sides of RMP sheet, which make up the top of fermenter, are in tubular shape, so that PVC pipes may be inserted inside them to give extra strength. The strengthened

sheet is then fixed to the wall of the fermenter with hooks.

The hydraulic retention time (HRT) is calculated according to the amount of water used to wash the pig houses, as the following the formula:

$$\text{HRT} = \frac{\text{Volume of fermenter}}{\text{Volume daily (manure + washing water)}}$$

A 1:3 ratio of manure to washing water is suggested, which can easily be achieved with a flushing tank system. According to the work by Hong (1985), the daily excreta of a 100-kg pig is around 5 liters, so the total wastewater from one pig may be estimated as 20 liters. A HRT of 12-15 days is common for hog wastewater treatment.

A tent-type fermenter should consist of no fewer than two digesters. The volume of the first digester is usually 1.2 times of the daily wastewater. Both acidogenesis and sedimentation take place in this first digester. Most of the methanogenesis reaction occurs in the rear digester(s). Biogas may be collected for the use as fuel. The excreta of each pig can generate 0.1-0.3 m³ of biogas per day. Biogas may be used in cooking stoves, water heaters, water pumps, electric power generators, gas lamps, warming piglets, vehicles, mowers, and incinerators for animal bodies, etc.

2.2.3 Aerobic Treatment

There are many kinds of aerobic treatments that may be utilized for livestock wastewater. Considering the environmental conditions of Taiwan in subtropical climate, activated sludge processing and oxidation ditches are recommended. In aerobic treatment, organic matter is decomposed solely through aerobic oxidation.

Activated sludge processes are versatile and flexible. Effluent of any desired quality can be produced by varying the processing parameters. These

processes require less land but more skilled management than simpler processes, such as oxidation ditches. Activated sludge is a complex biological mass, resulting from when organic wastes are aerobically treated. The sludge will contain a variety of heterotrophic microorganisms, including bacteria, protozoa, and higher forms of life. The relative abundance of any particular microbial species will depend on the type of waste that is being treated, and the way in which the process is operated. For optimum treatment, raw waste must be balanced nutritionally. In three-step treatment, most of the easily biodegradable matter has already been decomposed in the anaerobic digester, therefore, operating an activated sludge treatment requires intensive care for good performance. It is better to control the BOD of anaerobic effluent at around 1000 mg/L. The growth conditions for microorganisms in activated sludge tanks are usually measured according to the mixed liquor suspended solids (MLSS) and sludge volume index (SVI). The HRT for an aerobic tank is normally 1.0-1.5 days.

While activated sludge tanks have a water depth of 2-5 m, this should not exceed 1.5 m in oxidation ditches. Oxidation ditches, therefore, require a larger land area, but have the advantages of being easy to operate and of generating less sludge.

A final clarifier to settle the activated sludge before the discharge of treated water is required in aerobic treatment. The settled sludge may be removed by mechanical methods for return to the aerobic unit, or be dehydrated for disposal. Usually the HRT in the clarifier should not exceed 6 hours.

2.3 Utilization of Biogas

Biogas from the anaerobic tank contains very high degree of hydrogen

sulfide (H_2S), which can corrupt the power generator, so the desulfurization process is needed. The common method for reduction of hydrogen sulfide is biological desulfurization. In the process, the H_2S is absorbed in water and then its content is mitigated greatly by biological method. After desulfurization process, the humidity of biogas is very high due to the usage of water in such process. In this project, the biogas will pass through the active carbon tower to absorb water vapor in the biogas, then, this dehumidified biogas will store in a red plastic bag.

After above processes, biogas can be used either for the production of heat only or for the generation of electric power. Normally heat and power are produced in the same time for higher efficiency. Such power generators are called combined heat and power (CHP) generation plants, and normally use a four-stroke or a Diesel engine. A Stirling engine or gas turbine, a micro gas turbine, high- and low- temperature fuel cells, or a combination of a high-temperature fuel cell with a gas turbine are alternatives.

Biogas can also be used by burning it to produce steam, by which can drive an engine in the Organic Rankine Cycle (ORC) or the Cheng Cycle, the steam turbine, the steam piston engine, or the steam screw engine.

Figure 2.1 shows the range of capacities for the power generators, which are available on the market for the pilot-plant or industrial scale. The efficiency is defined as the ratio of the electrical power generated to the total energy content in the biogas. Efficiency figures are also provided by different manufacturers. Small-capacity engines generally can result in the lower efficiencies than that of high-capacity engines.

The generated current and heat can supply to the bioreactor itself, associated buildings, and neighboring industrial companies or houses. The power can be

fed into the public electricity network, and the heat into the network for long-distance heat supply. Vehicles can sometimes be driven by the power or the heat.

2.4 Engines

Figure 2.2 lists some engines that can be operated with biogas. These have been improved during the recent years by following the development works inspired by the worldwide boom in biogas plants. The performance by some manufacturers even has already exceeded that of those given in this figures.

2.4.1 Four-stroke Gas Engine and Diesel Engine

Today's four-stroke biogas engines were originally developed for natural gas and are therefore well adapted by the special features of biogas. Their electrical efficiencies normally do not exceed 34~ 40%, as the nitrogen oxide (NO_x) output has to be kept below the prescribed values. The capacity of the engines ranges from 100 KW to 1 MW.

Four-stroke biogas engines often run in the lean-burn range (ignition window $1.3 < \lambda < 1.6$, $\lambda = \text{air-fuel ratio/stoichiometric air-fuel ratio}$), where the efficiency is expected to drop. The efficiency of lean-burn engines with turbocharger is 33~ 39%. The NO_x emissions can be reduced, however, by a factor of 4 in comparison to ignition (by compression) oil Diesel engines, and the limiting values can be met without further measures. Since the engines tend to knock with varying gas qualities, a methane content of at least 45% in biogas should be ensured.

In small agricultural plants, ignition oil Diesel engines are frequently installed. These engines are more economical and have a higher efficiency than four-stroke engines in the lower capacity range. However, higher NO_x

emissions are produced by Diesel engine. Their lifetimes usually are given as 35,000h of operation.

In general, Diesel engines burning gas fuel can be operated by direct injection because pre-chamber engines develop hot places, resulting in uncontrolled spark failures with biogas. Owing to the internal formation of gas mixtures, Diesel engines can be faster controlled. The ignition oil Diesel engine is operated ideally at $\lambda < 1.9$. The efficiency is then up to 15% better than that in a four-stroke engine.

2.4.2 Stirling Engine

An alternative to the commonly used four-stroke and the Diesel engines is the Stirling engine. The efficiency of the Stirling process is closest to that of the ideal cycle. The Stirling engine has been recommended for power generation for many years, but is seldom realized on an industrial scale because of technical problems in details. Power generated from biogas in Stirling engines is not known yet in industrial scale installations.

2.4.3 Gas Turbine

Biogas can be converted to current via gas turbines of medium and large capacity (20 MW and more) at a maximum temperature 1200 °C. The tendency is to go to even higher temperatures and pressures, whereby the electrical capacity and thus the efficiency can be increased. The main parts of a gas turbine are the compressor, combustion chamber, and turbine.

Ambient air is sucked and compressed in the compressor and transmitted to the combustion chamber, where biogas is introduced and burnt with the compressed air. The flue gas that is so formed is passed to a turbine, where it expands and transfers its energy to the turbine. The turbine propels the compressor on the one hand and the power generator on the other hand. The

exhaust gas leaves the turbine at a temperature of approximately 400~600 °C. The waste heat can be recovered by driving a steam turbine downstream for heating purposes or for preheating the air that is sucked in.

2.4.4 Micro Gas Turbine

Micro gas turbines are small high-speed gas turbines with low combustion chamber pressures and temperatures. They are designed to deliver up to 200 kW electrical powers. For normal operation, the compressor sucks in the combustion air. The fuel is normally supplied to meet the combustion air in the combustion chamber. When biogas with a low calorific value is used, it must be adjusted to a flammable mixture of biogas and air before it is supplied into the combustion chamber.

The electrical efficiency of 15~25% for today's micro gas turbines is still unsatisfactorily low. An attempt to increase the efficiency has been made by preheating the combustion air in heat exchange with the hot turbine exhaust gases. But great improvements are still necessary before micro gas turbines can be introduced into the market of industrial biogas plants. However, the coupling of a micro gas turbine with a micro steam turbine to form a micro gas-steam turbine seems already interesting and economical today because of its high electrical efficiency.

2.4.5 Fuel Cell

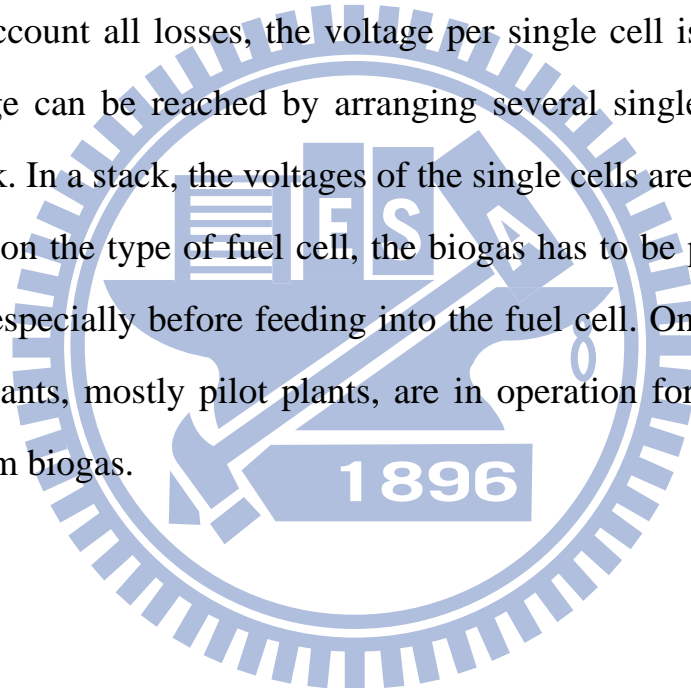
Comparing to combustion engines, the fuel cell converts the chemical energy of hydrogen and oxygen directly into current and heat. Water is formed as the reaction product.

In principle, a fuel cell works with a liquid or solid electrolyte held between two porous electrodes—anode and cathode. The electrolyte lets ions pass only and allow no free electrons from the anode to the cathode side. The electrolyte

is thus “electrically non-conductive.” It separates the reaction partners and thereby prevents direct chemical reaction. For some fuel cells, the electrolyte is also permeable to oxygen molecules. In this case the reaction occurs on the anode side. The electrodes are connected by an electrical wire.

Both reaction partners are continuously fed to the two electrodes, respectively. The molecules of the reactants are converted into ions by the catalytic effect of the electrodes. The ions pass through the electrolyte, while the electrons flow through the electric circuit from the anode to the cathode. Taking into account all losses, the voltage per single cell is 0.6 ~ 0.9 V. The desired voltage can be reached by arranging several single cells in series, a so-called stack. In a stack, the voltages of the single cells are added.

Depending on the type of fuel cell, the biogas has to be purified to remove CO and H₂S especially before feeding into the fuel cell. Only a small number of fuel cell plants, mostly pilot plants, are in operation for the generation of electricity from biogas.



Chapter 3

Experimental Apparatus and Procedures

3.1 Experiment layout

The Experiment layout is shown in Figure 3.1a. When the engine starts, the air and the biogas are sucked into the engine. The flow meters, marked by F1 and F2, measure the air and the biogas flow rates, which are controlled by valves at the engine inlets. The engine gets the power by combustion to drive the generator to produce the electricity. The thermocouple at the engine outlet measures waste gas temperature, and followed by the waste gas analyzer.

Figure 3.1b is the waste heat recovery system. The heat exchanger is installed following the exhaust pipe. The waste gases flow into the exchanger and transfer heat to intake gases (the mixture of biogas and air) in a separated pipe. We can control intake gas temperature by using a valve, located at the exchanger inlet, to regulate the amount of inlet gas into the heat exchanger. Part of inlet gas pass through the heat exchanger, another part of inlet gas flow into the engine directly. There are four thermocouples established at exchanger inlets and outlets. T1 and T2 measure the temperatures of waste gases before and after the heat exchanger. T3 and T4 are for inlet gas temperatures at inlet and outlet.

3.1.1 Engine

The original four-stroke diesel engine was operated with diesel fuel, using compression to ignite the fuel. In order to use biogas gas as fuel, the spark ignition system was installed to the engine. In other words, The ignition way was changed into spark ignition instead of comprssion one. For the original engine, the ideal power cycle is Diesel cycle. When the compression ignition

system is converted to spark ignition system, the ideal power cycle of present engine becomes Otto cycle. Figure 3.2 shows the refurbished engine and its detailed data can be referred in the following table.

Table 3.1 Engine Technical Data

Engine Technical Data	
Engine model	8031i06
Diesel 4 stroke - Injection type	direct
N° of cylinders	3 in line
Total displacement	2.9 L
Bore x Stroke	104 x 115 mm
Compression ratio	10 : 1
Aspiration	natural
Cooling system	liquid (water + 50% Paraflu11)
Lube oil specifications	ACEA E2-96 MIL-L-2104E
Lube oil consumption	~ 0.3% of fuel consumption
Fuel specifications	EN 590
Speed governor	mechanical (G2 class)
Engine rotating mass moment of inertia	0.942 kg m ²
Dry weight (standard configuration)	~ 370 kg

3.1.2 Air Flow Meter (VA-400)

The flow meter at air inlet is insertion type VA-400 flow sensor, whose range varies with the installed pipe diameter. In order to maintain the accuracy stipulated in the data sheets, the sensor must be inserted in the center of a

straight pipe section with an undisturbed flow progression. An undisturbed flow progression is achieved if the sections in front of the sensor and behind the sensor are sufficiently long, absolutely straight and without any obstructions such as edges, seams, curves etc. The minimum length ahead the sensor along the pipe should be 10 times of pipe diameter and 5 times behind sensor for the fully developed turbulent flow profile, so the measured flow rate can be accurate enough. Figures 3.3a and 3.3b show the flow meter and its detailed data.

3.1.3 Biogas Flow Meter (TF-4000)

The flow meter at biogas inlet is TF-4000 thermal-mass flow meter. Figure 3.4a and Figure 3.4b show the flow meter and its technical data. Operation principle is following: Two temperature sensors are put on along the flow path of gas. One of them is heated by a controlled power supply, and another one is not heated. The temperature difference between these two sensors should be always kept constant under a fixed mass flow rate. The different mass flow rate will result in different temperature difference. Therefore, it can deduce the mass flow rate of fluid flow by the quantity of power supply to maintain the temperature difference between these two sensors.

3.1.4 Thermocouple

A thermocouple is a sensor for measuring temperature. It consists of two dissimilar metals joined together at one end, which can produce a small unique voltage at a given temperature. This voltage is measured and interpreted by a thermometer. Thermocouples are available in different combinations of metals or calibrations. The four most common calibrations are J, K, T and E. Each calibration has a different temperature range and environment.

Type K (Chromel–Alumel) is the most commonly used thermocouple with a

sensitivity approximately $41 \mu\text{V}/^\circ\text{C}$. The voltage of Chromel is positive relative to the one of alumel. It is inexpensive and its temperature is wide, ranging from -200°C to $+1350^\circ\text{C}$.

In this research, four K-type thermocouples is used for measuring waste gas temperature and inlet gas temperature. Figure 3.5 shows the picture of K-type thermocouple.

3.1.5 Gas Analyzer (HM5000)

Figure 3.6 is the gas analyzer, HM5000, used for measuring waste gas component data, which include the concentrations of oxygen, NO_x and carbon dioxide.

3.1.6 Methane Concentration Analyzer

Figure 3.7 is guardian plus infra-red gas monitor, which is used for measuring the methane concentration of the inlet biogas.

3.1.7 Heat Exchanger

The heat exchanger (see Figure 3.8) is placed at waste gas outlet to heat the inlet gases. It consists of many small pipes of intake gases to enhance the heat transfer between the hot waste and inlet gases. The void space between the casting and pipes is for the passage of waste gases.

3.1.8 Data Acquisition

Data acquisition system can automatically collect signals from analog and digital measurement sources, such as sensors and devices, under tests. It uses a combination of PC-based measurement hardware and software to provide a flexible and user-defined measurement system. Usually, the researcher must calibrate sensors and signals before a data acquisition device acquires them. The specifications of these modules of National Instruments are shown in Table 3.2.

Table 3.2 Specifications of the Data Acquisition Modules

Model	Signal Type	Channels	Max Sampling Rate	Resolution	Signal Input Ranges
NI 9203	Current	8	500 k/s	16 bits	±20 mA
NI 9211	Thermocouple	4	15 k/s	24 bits	±80 mV

National Instruments, a leader in PC-based data acquisition, offers a complete family of proven data acquisition hardware devices and the powerful and easy-to-use software that can extend to many languages and operating systems. NI CompactDAQ delivers fast and accurate measurements in a small, simple, and affordable system. A CompactDAQ Chassis shown in Figure 3.9a, a product of NI, is adopted because of the following advantages: plug-and-play installation and configuration, AC power supply and USB cable connection, mounting kits available for panel, enclosure, DIN-rail and desktop development, A380 metal construction, more than 5 MS/s streaming analog input per chassis, and Hi-Speed USB-compliant connectivity to PC. Different types of signal process modules are chosen to complete the data acquisition system, including NI 9203 Analog Input Module, NI 9211 Thermocouple Differential Analog Input Module. Both are shown in Figure 3.9b and Figure 3.9c.

3.1.9 Temperature Monitor

Four k-type thermalcouples are installed to the temperature monitor (see Figure 3.10). The temperature variation can be seen and recorded by the monitor.

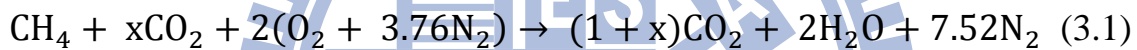
3.1.10 Humidity Temperature Meter (Center 311)

The Center 311 humidity temperature meter is shown in Figure 3.11. It is used to measure the humidity and temperatures of the environment and biogas.

3.2 The Theoretical Calculation

The following calculations include excess air ratio, thermal efficiency, theoretical mole fraction of CO₂ in waste gas and theoretical percentage of consumed CH₄. These will be used in the analyses of the following experiments.

The air-fuel ratio (AF) is defined as a ratio of the mole of air to the one of fuel in the combustion process. The stoichiometric reaction for combustion of methane with standard air is given as:



where x is the moles of CO₂ in the biogas. The stoichiometric air-fuel ratio, AF_{stoich}, is:

$$\text{AF}_{\text{stoich}} = \frac{\text{mole of air}}{\text{mole of methane} + \text{mole of CO}_2} = \frac{2 \times 4.76 \text{ mole}}{(1+x) \text{ mole}} \quad (3.2)$$

On the other hand, AF_{act} is the air-fuel ratio of the actual mole of air to mole of methane into the engine. Because the mole ratio is equal to the volume flow rate ratio, and the methane flow rate is equal to the biogas flow rate multiplying methane mole fraction in the biogas. AF_{act} can be also expressed as:

$$\begin{aligned} \text{AF}_{\text{act}} &= \frac{(\text{mole of air})_{\text{act}}}{(\text{mole of methane} + \text{mole of CO}_2)_{\text{act}}} = \frac{\text{Air flow rate}}{\text{Methane flow rate} + \text{CO}_2 \text{ flow rate}} \\ &= \frac{\text{Air flow rate}}{\text{Biogas flow rate}} \quad (3.3) \end{aligned}$$

If the methane concentration of biogas is 73%, then the CO₂ concentration of biogas is assigned as 27%:

$$x = 0.369, \text{AF}_{\text{stoich}} = \frac{2 \times 4.76 \text{ mole}}{(1+0.369) \text{ mole}} = 6.95$$

The air flow rate can be measured by air flow meter directly, whereas the methane flow rate is obtained by the measured biogas flow rate multiplied by the mole fraction of methane (both flow meters were demonstrated in sections 3.1.2 and 3.1.3). An example is given as follows: If the air and biogas flow rate were measured as 1400 and 240 liters per minute, respectively, then, the actual air-fuel ratio with 73% CH₄ is:

$$\text{AF}_{\text{act}} = \frac{1400\text{L}/\text{min}}{240\text{L}/\text{min}} = 5.83 \quad (3.4)$$

The *Excess Air Ratio* (λ) is the ratio of the actual mole of air used to the stoichiometric mole of air, defined as:

$$\lambda = \frac{(\text{mole of air})_{\text{act}}}{(\text{mole of air})_{\text{stoich}}} = \frac{\left(\frac{\text{mole of air}}{\text{mole of fuel}}\right)_{\text{act}}}{\left(\frac{\text{mole of air}}{\text{mole of fuel}}\right)_{\text{stoich}}} = \frac{\text{AF}_{\text{act}}}{\text{AF}_{\text{stoich}}} \quad (3.5)$$

Note that the actual mole of fuel is equal to stoichiometric mole of fuel because in the engine experiments the fuel supply rate is fixed, whereas the air volume flow rate is changed. As a consequence, the excess air ratio is equal to ratio of AF_{act} to AF_{stoich}. Also remind that λ is reciprocal of equivalence ratio.

From those definitions, the resultant *Excess Air Ratio* (λ) for the above example is

$$\text{Excess Air Ratio} = \frac{AF_{\text{act}}}{AF_{\text{stoich}}} = \frac{5.83}{6.95} = 0.83 \quad (3.6)$$

The thermal efficiency is calculated for how much energy converting into electric power, its formulation is as following :

$$\text{Thermal Efficiency} = \frac{\text{Power Generation}}{\text{Energy Input}} \quad (3.7)$$

where *Energy Input* is calculated from the lower heating value (LHV) of methane, whose value is 50020kJ/kg, in the biogas. It is expressed as:

$$\text{Energy Input} = \dot{m}_{\text{CH}_4} \times \text{LHV of CH}_4 \quad (3.8)$$

The power generation of this study is the power output of biogas generator. When the engine push the generator to work, there are many heat loss between the generator and engine, so the exact power output of engine is impossible to calculate.

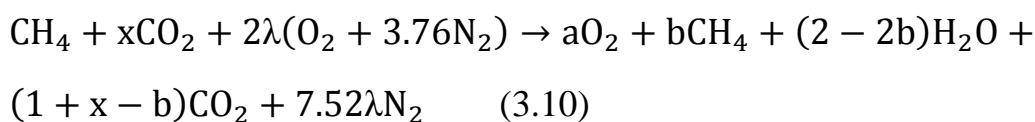
Where \dot{m}_{CH_4} is the methane mass flow rate in biogas, and it is calculated by:

$$\dot{m}_{\text{CH}_4} = \text{biogas flow rate} \times \text{CH}_4\% \times \rho_{\text{CH}_4} \quad (3.9)$$

where ρ_{CH_4} is the density of methane, which is 0.717 kg/m³ at STP.

The theoretical consumed percentage of CH₄ and the percentage of CO₂ in waste gas in the combustion process are calculated as follows:

The balanced reaction is:



where the NO_x concentration (in an order of ppm) in waste gas can be neglected. x is the moles of CO_2 in the biogas, and a and b are the moles of O_2 and CH_4 , respectively, in waste gas. a can be calculated from the percent of O_2 in waste gas as follow:

$$\text{mole fraction (\%)} \text{ of } \text{O}_2 = \frac{a}{1+x+9.52\lambda} \quad (3.11)$$

where $1 + x + 9.52\lambda$ is the total moles in waste gas, b is obtained from the atom balance as:

$$b = 1 - \lambda + \frac{a}{2} \quad (3.12)$$

The theoretical percent of CO_2 in waste gas can be calculated by:

$$\textit{Theoretic mole fraction of } \text{CO}_2 (\%) = \frac{1+x-b}{1+x+9.52\lambda} \quad (3.13)$$

The theoretical percent of used CH_4 is defined as:

$$\textit{Theoretical percentage of consumed } \text{CH}_4 (\%) = \frac{(\text{CH}_4)_{\text{in}} - (\text{CH}_4)_{\text{out}}}{(\text{CH}_4)_{\text{in}}} \quad (3.14)$$

3.3 The Effect of Methane Concentration

The methane concentration of biogas can be affected by the organics concentration in wastewater. The variation of methane concentration will make impact on the generator performance. In order to gain a higher thermal efficiency, it is important to find the optimum excess air ratio under different methane concentration. The collected data are expected to be used for the long-term electricity generation.

The experimental parameters include methane concentration of biogas, biogas flow rate and excess air ratio. Before experiment, the methane concentration of biogas is measured. The biogas flow rates are set as 140, 160, 180, 200, 220, 240 and 260L/min, respectively. Under each fixed biogas flow rate, it tests different excess air ratios, ranged from 0.8 to 1.6. The collected data include biogas flow rate, air flow rate, power generation, waste gas temperature, methane concentration, oxygen concentration, carbon dioxide concentration and NO_x concentration. The measurement starts when the engine is operating continuously until all conditions are ensured to be steady. Then, all measurements were tested twice and took an average. The experimental procedure is as follows:

1. Measure the methane concentration of biogas.
2. Operate the engine at least 20 minutes so it would be steady.
3. Fix the biogas flow rate at demanded quantity.
4. Control the air flow rate for specific excess air ratio.
5. Collect the corresponding data, mentioned above.
6. Repeat the procedure for different excess air ratio.
7. Repeat the above procedure for different methane concentration.

3.4 The Effect of Intake Gases Temperature

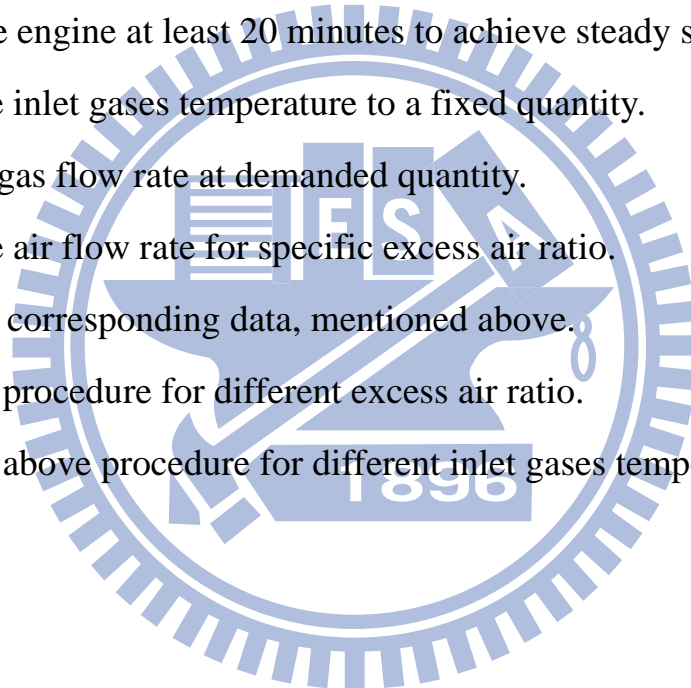
Preheating the inlet gas (the mixture of biogas and air) to different temperatures before the mixture gas enters the engine can increase the combustion efficiency. The measurements and controlling strategy are given previously.

The experimental parameters are inlet gases temperature, biogas flow rate and excess air ratio. The biogas flow rates are 140, 160, and 180 L/min, and

the excess air ratios ranged from 0.8 to 1.6. Under each fixed inlet gases temperature, it tests different biogas flow rates and each of it is accompanied with different excess air ratios.

After the engine is operated steadily, and collect the data include inlet gases temperature, waste gas temperature, biogas flow rate, air flow rate and power output. The experimental procedure is as follows:

1. Measure the methane concentration of biogas.
2. Set up heat exchanger at waste gas outlet.
3. Operate the engine at least 20 minutes to achieve steady state.
4. Control the inlet gases temperature to a fixed quantity.
5. Fix the biogas flow rate at demanded quantity.
6. Control the air flow rate for specific excess air ratio.
7. Collect the corresponding data, mentioned above.
8. Repeat the procedure for different excess air ratio.
9. Repeat the above procedure for different inlet gases temperature.



Chapter 4

Results and Discussion

This study is a continuous effort of Lin's work [3], which carried out the electricity generation of the subproject 2 in a small swine farm in Miaoli. Now, this project was moved to Taiwan Sugar swine farm in Taichung, whose size was about 1.5 times of that in Miaoli.

The biogas used in this research was supplied from the anaerobic tank made of red plastic bag. The high concentration of H_2S existed in the original biogas was expected to corrode the engine, so the H_2S removal system was set up in subproject 1 by Tseng and his colleagues [25]. The H_2S concentration in the biogas was effectively reduced from 4000 to 300ppm. The resultant desulfurized biogas passed a methane concentration analyzer, and the measurement found that it comprised about 50~75% of CH_4 and 20%~30% of CO_2 mainly. Then, the engine operated with the desulfurized biogas as fuel and generated electric power for farm usage. In the following experiments, the concentration of CH_4 is fixed at 73% (obtained by measurement) approximately, and the other gases are lumped as CO_2 since it is the major component other than CH_4 .

4.1 Effect of Excess Air Ratio (λ)

The excess air ratio (λ), a reciprocal of equivalence ratio (ϕ), was defined in Eq. (3.5) of Section 3.2. $\lambda=1$ represents the stoichiometric condition. When $\lambda>1$, it means the mixture is fuel-lean, and $\lambda<1$, the mixture is fuel-rich.

The biogas supply rates in this research were ranged from 140 to 260 liters per minute and the corresponding excess air ratios were from 0.8 to 1.6. Note

that the maximum allowable total volume flow rate (sum of biogas and air flow rates) into the engine is about 1800 L/min, therefore, the maximum air supply rate is limited by the biogas supplied flow rate. In other words, the experiments with the higher biogas flow rate carried out with a narrower range of air flow supply rate. So it restricted the maximum excess air ratio for each biogas supply rate. Such limitations in experiments are summarized in the following Table.

Table 4.1 Limiting Value of Air Supply for Each Biogas Supply Rate

Biogas Flow Rate (L/min)	140	160	180	200	220	240	260
Max. Air Flow Rate (L/min)	1540	1600	1600	1530	1520	1500	1520
λ_{\max}	1.58	1.43	1.27	1.1	0.99	0.89	0.84

The detailed resultant experimental data for each specified biogas flow rate are given in Table 4.2a~g. In these tables, the measured results include the power generation, waste gas temperature and waste gas species concentrations (O_2 , CO_2 and NO_x). In addition, the thermal efficiency, CH_4 consumption and CO_2 concentration deduced from measurements described in Sec. 3.2 are provided as well.

Figures 4.1 is the power generation as a function of excess ratio ratio at different biogas supply rates with 73% methane concentration. From the data of 140L/min of biogas flow rate, it seems provide a complete flammability domain between the upper and lower limits, which are $\lambda = 0.8$ (equivalent to $\phi = 1.25$) and $\lambda = 1.58$ (equivalent to $\phi = 0.63$), respectively. At standard

atmospheric pressure and temperature, in a vertical glass tube, the flammability limits of pure methane are $\phi = 0.5$ and $\phi = 1.68$. Increasing pressure above atmospheric pressure usually widens the flammability range. Most of the widening occurs at the fuel-rich side, the flammability limits on the fuel-lean side is not strongly pressure-dependent [27]. When the combustion occurs in engine, the pressure is higher than standard atmospheric pressure. In theory, the flammability range should be wider. However, in this study, it has a narrower flammability range, due to following reasons. First, 73% CH_4 of biogas was used as fuel instead of pure methane. The CO_2 in the biogas act as dilution would absorb part of heat energy, so the flammability range is narrower. Secondly, the flammability range is deduced by the operation range of engine, instead of real air-fuel limit of flame propagation. The mechanical structure of engine is more complicated than glass tube, so the heat loss is higher than that of glass tube. This heat loss of engine makes flammability range become narrower. Due to above reasons, the present biogas with 73% of CH_4 is as expected to have a narrower flammability range. As the biogas flow rate increases, the lower flammability limits in terms of ϕ are no longer achieved due to the restricted air supply rate, mentioned previously. On the other hands, the upper one still can be maintained as a fixed vale of $\lambda = 0.8$ (or $\phi = 1.25$).

From the case of 140L/min biogas flow rate, the optimal excess air ratio occurs at $\lambda = 1.2$ (or $\phi = 0.83$) with a maximumu power of 12.9kW. In the case of 160L/min, the optimum is $\lambda = 1.29$ (or $\phi = 0.77$) with a maximumu power of 16.4kW. The optimal λ no longer can be obtained as the biogas flow rate

increases further for this engine. Therefore, the engine can be operated at the part of fuel-lean regime from 160~200 L/min of biogas supply rates. For the biogas supply rate greater than 200 L/min, it can only operate at fuel rich regime, where the generated power increases with an increase of excess air ratio.

It can be seen that at a given excess air ratio, the higher the biogas supply rate, the higher the power generation. The maximum power output that the present engine can achieve is 26.7 kW at biogas supply of 260 L/min with an excess air ratio of 0.84. However, its corresponding thermal efficiency is 0.235; see Fig. 4.2 (the deduced thermal efficiency verse λ), which is not the highest one. It is because of the limited air supply, unable to lead to the optimal λ . The maximum thermal efficiency is 0.27 occurred at the biogas supply rate of 200 L/min with $\lambda= 1.1$.

In general, the trends for both Figs. 4.1 and 4.2 are quite similar, since the thermal efficiency is directly proportional to power generation (see Eq. (3.7) in Section 3.2) for each fuel flow rate.

The biogas supply rate affects the optimal λ , behind which the performance starts to decline as discussed previously. When the biogas supply rates are above 180L/min, under each fixed biogas flow rate, the power generation and thermal efficiency increase with an increase of excess air ratio. When the biogas supply rates are below 180L/min, the lower biogas supply rate is given, the smaller optimal excess air ratio λ . This is because the total heat energy released from the combustion process is less at lower biogas supply rate. For the case of 160L/min, the power and thermal efficiency start to descend at $\lambda =1.29$. For the case of 140L/min, they even starts to descend at $\lambda =1.20$.

The results show that the engine can produce higher power and greater

thermal efficiency with higher biogas supply rates with larger excess air ratios, but maximum inlet gas flow rate of engine limits these trends to increase.

Figure 4.3 shows the waste gas (or flue) temperatures for different biogas supply rates as a function of excess air ratio. Similar to the power generation and thermal efficiency, the exhaust temperature is higher as the biogas supply rate is higher at a specified excess air ratio. It is because more heat can be released in combustion when biogas supply rate increases, leading to the higher waste gas temperature. Also the maximum waste gas temperatures occurs at $\lambda=0.9\sim 1.1$ (near stoichiometric condition) except the ones of 240 and 260L/min biogas supply rates, which cannot reach the stoichiometric condition.

Figures 4.4, 4.5 and 4.6 are the O_2 , CO_2 and NO_x concentrations in the waste gas at different biogas supply rates as a function of excessive air ratio. These data are presented in the row 6, 7 and 8 in Table 4.1 a~g as well. In Fig. 4.4, the O_2 concentration in flue gas increase with increasing excess air ratio, because more O_2 is left during combustion as the air supply increases. The CO_2 concentration in Fig.4.5 generally decreases with increasing excess air ratio, except the cases for biogas supply rates of 180, 200 and 220L/min, which have the peak values at $\lambda=0.9$. Remind that it already exists approximately 27% of CO_2 in the biogas gas supplied. The extra CO_2 is from combustion. When the combustion is more completed, such around $\lambda=0.9$, the generated CO_2 can outweigh the dilution effect by other combustion product gases, leading to a peak appearance near stoichiometric condition. In Fig. 4.6, the NO_x concentration reaches to peak value in the range around $\lambda=0.9\sim 1.1$ (near stoichiometric condition) that is coincident with the waste gas temperature of Fig. 4.3, indicating that the main source of NO_x is from thermal NO_x .

This study applies the measured O_2 data in the waste gas to estimate the corresponding CO_2 concentration and the consumed percentage of CH_4 . They are derived by using Eqs. (3.13) and (3.14). The consumption percentage of CH_4 in combustion and the corresponding estimated CO_2 concentration are presented in the tenth and eleventh rows of Table 4.1 a~g, respectively. The maximum discrepancy of CO_2 concentration between the estimations and the ones measured by the gas analyzer are around 3%, showing that the agreements are quite well.

Figure 4.7 shows the deduced CH_4 consumption ratio as a function of excess air ratios. It can be seen that the maximum consumption ratio occurs in the neighborhood of stoichiometric ratio ($0.9 < \lambda < 1.1$), then it descends toward the upper and lower flammability limits. The highest CH_4 consumption ratio is 96.03% at biogas supply rate of 200L/min with $\lambda=1.1$, consistent with highest thermal efficiency (see Fig.4.2).

To sum up, the optimum biogas supply rate to the present engine with 73% CH_4 of biogas seems to be 200 L/min because it has the highest thermal efficiency and the highest CH_4 consumption ratio. However, it cannot provide the maximal power output (26.7kW), which occurs at biogas supply rate of 260L/min with $\lambda= 0.84$.

Table 4.2a Power Generation Rates as A Function of Excess Air Ratio at
Biogas Volume Flow Rate 140L/min

Biogas supply at 140L/min									
Air flow (L/min)	780	870	970	1070	1170	1260	1360	1460	1540
Excess air ratio	0.8	0.89	0.99	1.09	1.2	1.29	1.39	1.50	1.58
Power (kWe)	7.6	9.8	11.8	12	12.9	12.7	12.4	11.5	7.3
Thermal efficiency	0.124	0.160	0.193	0.196	0.211	0.207	0.202	0.188	0.119
Waste gas temperature (°C)	401.9	412.9	427.5	422.8	421.7	420.5	407.5	400.8	348.5
O ₂ (%)	1.67	1.66	2.77	4.04	5.4	7.38	8.68	12.03	13.48
NO _x (ppm)	332	1308	1077	705	304	177	0	0	0
CO ₂ (%)	13.23	12.89	12.02	10.99	10.18	9.43	8.89	8.32	8.13
Estimation values									
Used CH ₄ (%)	72.65	81.21	84.65	86.05	85.64	78.95	76.08	55.89	47.48
CO ₂ (%)	12.17	11.96	11.19	10.39	9.56	8.46	7.70	5.93	5.13

Table 4.2b Power Generation Rates as A Function of Excess Air Ratio at
Biogas Volume Flow Rate 160L/min

Biogas supply at 160L/min								
Air flow (L/min)	890	1000	1110	1220	1330	1440	1550	1600
Excess air ratio	0.8	0.89	0.99	1.09	1.19	1.29	1.39	1.43
Power (kWe)	9	12.9	15	15.3	15.6	16.4	16.3	16.1
Thermal efficiency	0.128	0.184	0.214	0.219	0.223	0.234	0.233	0.230
Waste gas temperature (°C)	426.3	451.6	464.1	457.2	449.1	440.6	431	419.4
O ₂ (%)	1.25	2.06	2.44	3.76	4.97	6	7.67	9.73
NO _x (ppm)	518	1362	1286	966	740	250	20	0
CO ₂ (%)	13.89	13.39	12.76	11.8	10.76	9.8	8.75	8.63
Estimation values								
Used CH ₄ (%)	74.42	79.70	86.56	87.50	87.91	88.40	83.25	70.58
CO ₂ (%)	12.39	11.74	11.36	10.53	9.79	9.15	8.21	7.13

Table 4.2c Power Generation Rates as A Function of Excess Air Ratio at Biogas Volume Flow Rate 180L/min

Biogas supply at 180L/min						
Air flow (L/min)	1000	1120	1250	1370	1500	1600
Excess air ratio	0.79	0.89	0.99	1.09	1.19	1.27
Power (kWe)	10.8	16.1	17.3	18.5	19.2	19.3
Thermal efficiency	0.137	0.204	0.220	0.235	0.244	0.245
Waste gas temperature (°C)	461.3	477.7	480.5	487.6	480.8	478.1
O ₂ (%)	1.09	1.06	1.95	3.05	4.67	5.68
NO _x (ppm)	111	854	1303	1040	857	353
CO ₂ (%)	13.5	13.8	12.89	12.46	11.23	9.73
Estimation values						
Used CH ₄ (%)	75.04	84.29	89.31	91.52	90.05	89.43
CO ₂ (%)	12.47	12.25	11.60	10.89	9.93	9.33

Table 4.2d Power Generation Rates as A Function of Excess Air Ratio at Biogas Volume Flow Rate 200L/min

Biogas supply at 200L/min				
Air flow (L/min)	1110	1250	1390	1530
Excess air ratio	0.79	0.89	1	1.1
Power (kWe)	14.5	18.7	20.6	23.6
Thermal efficiency	0.166	0.214	0.236	0.27
Waste gas temperature (°C)	476.8	498.7	515.9	516.8
O ₂ (%)	1.34	1.12	2.17	2.37
NO _x (ppm)	441	1090	1309	1111
CO ₂ (%)	13.92	14.08	13.46	12.7
Estimation values				
Used CH ₄ (%)	73.84	84.37	88.18	96.03
CO ₂ (%)	12.35	12.21	11.49	11.22

Table 4.2e Power Generation Rates as A Function of Excess Air Ratio at
Biogas Volume Flow Rate 220L/min

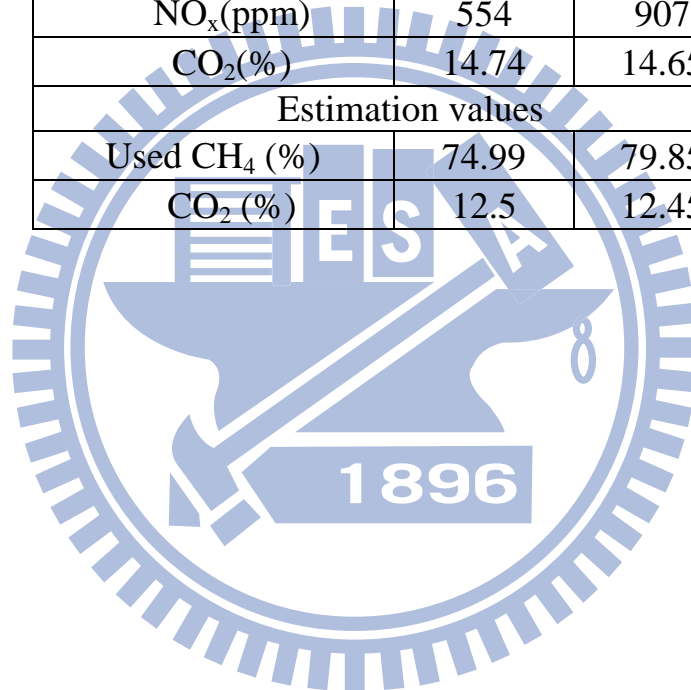
Biogas supply at 220L/min			
Air flow (L/min)	1220	1370	1520
Excess air ratio	0.79	0.89	0.99
Power (kWe)	17.5	21.5	24
Thermal efficiency	0.182	0.223	0.25
Waste gas temperature (°C)	492.4	518.2	526.1
O ₂ (%)	1.37	1.11	2.24
NO _x (ppm)	625	1440	1235
CO ₂ (%)	14.13	14.3	14.01
Estimation values			
Used CH ₄ (%)	73.65	84.11	87.28
CO ₂ (%)	12.33	12.23	11.46

Table 4.2f Power Generation Rates as A Function of Excess Air Ratio at
Biogas Volume Flow Rate 240L/min

Biogas supply at 240L/min		
Air flow (L/min)	1330	1500
Excess air ratio	0.79	0.89
Power (kWe)	19.8	25.4
Thermal efficiency	0.189	0.242
Waste gas temperature (°C)	514.5	538
O ₂ (%)	0.96	1.18
NO _x (ppm)	515	1255
CO ₂ (%)	14.8	14.57
Estimation values		
Used CH ₄ (%)	75.43	84.07
CO ₂ (%)	12.54	12.18

Table 4.2g Power Generation Rates as A Function of Excess Air Ratio at
Biogas Volume Flow Rate 260L/min

Biogas supply at 260L/min		
Air flow (L/min)	1440	1520
Excess air ratio	0.79	0.84
Power (kWe)	23.6	26.7
Thermal efficiency	0.208	0.235
Waste gas temperature (°C)	533.3	537.5
O ₂ (%)	1.05	0.91
NO _x (ppm)	554	907
CO ₂ (%)	14.74	14.65
Estimation values		
Used CH ₄ (%)	74.99	79.85
CO ₂ (%)	12.5	12.45



4.2 Effect of Methane Concentration

As mentioned before, the methane concentration of biogas can be affected by the organics concentration in wastewater. In the last year, Lin [3] tested different air-fuel ratio for 30kW generator with 60% methane concentration of biogas in a small swine farm in Miaoli. The results of Lin's research is given in Table 4.4a~e. In this table, under each fixed biogas flow rate, the results include the power generation, deduced thermal efficiency and waste gas temperature. In this year, the experimental tests used the same engine/generator but with 73% methane concentration of biogas in Taichung. Therefore, the comparison of using different methane concentrations is made in this section.

The power generation, deduced thermal efficiency and waste gas temperature for CH₄ concentrations of 60% and 73% are presented in Figs. 4.8~10, separately, in which the solid lines indicates the present results, whereas the dash line indicates the Lin's one [3]. Also remind that Lin's work cannot apply the biogas flow rates of 140 and 160L/min because the CH₄ concentration is too low to maintain the combustion in those biogas gas supply rates.

It is known by Eq. (3.5) of Section 3.2 when the methane concentration of biogas becomes higher under the same biogas supply rate, a higher air supply rate is needed in order to maintain a specific excess air ratio. In addition, the maximum allowable total volume flow rate (sum of biogas and air flow rates) into the engine is still retained that is about 1800L/min for the present engine. These two reasons further narrow down the range of the maximum excess air ratio. Table 4.3 shows the maximum excess air ratio of different biogas supply

rates with 60% and 73% CH₄ of biogas. Take biogas supply rate of 260L/min for example, the maximum λ is 1.01 with 60% methane concentration of biogas, whereas it is 0.84 with 73% methane concentration of biogas. For 200 L/min and 180L/min, the maximum excess air ratios with 73% CH₄ of biogas, 1.1 and 1.27, are greater than the ones, 1.09 and 1.13 with 60% CH₄ of biogas. This is because an increase of methane concentration in biogas can produce higher heat energy under the same biogas supply rate with enough air, and then the combustible range can be extended further. As a consequence, the lean misfire limit (maximum excess air ratio) is wider. This improvement can also be seen from Figs.4.8 and 4.9, which will be discussed later.

Table 4.3 The Maximum Excess Air Ratio of Biogas Flow Rate with 60% and 73% CH₄ of Biogas.

Biogas flow rate(L/min)	180	200	220	240	260
λ_{\max} (CH ₄ %)					
λ_{\max} (60%)	1.13	1.09	1.11	1.13	1.01
λ_{\max} (73%)	1.27	1.1	0.99	0.89	0.84

Figures 4.8 and 4.9 show the respective power generation and thermal efficiency under 60% and 73% methane concentration of biogas.

The results show that when the methane concentration rises from 60% to 73%, the trend of power generation and thermal efficiency change. With 60% CH₄ of biogas, the power generation and efficiency start to decay after $\lambda \approx 0.95$ for 200 and 220L/min. For 180 L/min, it even starts from the very beginning $\lambda=0.78$ to decrease. With 73% CH₄ of biogas, as mentioned in section 4.1, for the biogas supply rates above 180L/min, the power generation

and thermal efficiency increase with the increase of excess air ratio. As a result, for 180L/min (Fig. 4.8 and Fig. 4.9), it can be seen clearly that the lean misfire limit is widened from 1.13 to 1.27, when methane concentration of biogas increases from 60% to 73%.

In Figure 4.8, the power generation with 73% CH₄ of biogas are higher than the ones with 60% CH₄ of biogas, except the region around $\lambda < 0.85$. However, in Figure 4.9, the thermal efficiency increases with the increasing methane concentration just when the excess air ratio is greater than 0.95 (near stoichiometric condition). In the region of $\lambda > 0.95$, the thermal efficiencies with 73% CH₄ are more than the ones with 60% CH₄. The maximum difference can be achieved to about 11% at biogas supply rate of 180L/min. This improvement enlarges the lean misfire limit, mentioned above. For the mixture on the relatively rich side ($\lambda < 0.95$), there is no benefit. Moreover, in this region, the thermal efficiencies with 73% CH₄ are much less than the ones with 60% CH₄, and the maximum difference can be reached to about 7%. This is because incomplete combustion becomes serious in the fuel-rich region [11]. Besides, when the methane concentration increases, or when the excess air ratio decreases, where mixture becomes richer, the flame velocity is relatively faster comparing to lean mixture. It means that the spark timing should be delayed to avoid knocking, but the spark timing is fixed in this experiment. In order to get better performance, the ignition plug should ignite the mixture properly according to the position piston in the cylinder and the fuel/air ratio. If the ignition time advances too much, leading to engine knocking. If the ignition time delays too much, the combustion pressure acting on the piston will decrease, leading to a loss of efficiency.

It might conclude that the incomplete combustion and improper ignition

timing make the thermal efficiency not good as expected.

With 60% CH₄ of biogas, the maximum power generation and thermal efficiency are 26.8 kW and 0.287 at the same biogas supply rate of 260L/min with $\lambda=1.01$. On the other hand, with present 73% CH₄ of biogas, as mentioned before in Section 4.1, the maximum power generation and thermal efficiency occur at different biogas supply rates. The maximum power generation is 26.7 at biogas supply rate of 260L/min with $\lambda=0.84$, but the maximum thermal efficiency is 0.27 at biogas supply rate of 200L/min with $\lambda=1.1$. It indicates that different CH₄ concentrations of biogases will change the combustion characteristics for the same engine.

The comparison of waste gas temperature is showed in Figure 4.10. The waste gas temperature with 73% CH₄ of biogas is higher than the one with 60% CH₄, because the higher heat energy are produced with higher CH₄ concentration of biogas at the same biogas supply rate. So the waste gas temperature becomes higher. However, the increase of temperature with higher methane concentration does not mean the power generation and thermal efficiency increase, since the energy might be lost due to incomplete combustion and improper ignition timing.

To sum up, the rise of methane concentration can increase the power generation and thermal efficiency in the lean region. However, the the excess air ratio at higher biogas flow rate is restricted by allowable total volume of engine. Based on this reason, in order to get better engine performance, solving the problem of the limit excess air ratio for high biogas supply rate is needed.

Table 4.4a Power Generation Rates as A Function of Excess Air Ratio at
Biogas Volume Flow Rate 180L/min with 60% CH₄ [3]

Biogas supply at 180L/min					
Air flow (L/min)	800	910	960	1030	1160
Excess air ratio	0.78	0.89	0.93	1	1.13
Power (kWe)	13.6	13.5	13.1	11.9	8.5
Thermal efficiency	0.211	0.209	0.203	0.184	0.132
WasteGas temperature (°C)	459	460	465	466	450

Table 4.4b Power Generation Rates as A Function of Excess Air Ratio at
Biogas Volume Flow Rate 200L/min with 60% CH₄ [3]

Biogas supply at 200L/min					
Air flow (L/min)	910	1000	1080	1150	1250
Excess air ratio	0.8	0.875	0.943	1.01	1.09
Power (kWe)	16.2	16.6	16.5	15.3	13.8
Thermal Efficiency	0.226	0.231	0.230	0.213	0.192
Waste gas temperatre (°C)	474	473	474	476	472

Table 4.4c Power Generation Rates as A Function of Excess Air Ratio at
Biogas Volume Flow Rate 220L/min with 60% CH₄ [3]

Biogas supply at 220L/min					
Air flow (L/min)	1000	1100	1185	1250	1400
Excess air ratio	0.8	0.88	0.94	0.99	1.11
Power (kWe)	18.9	19.2	19.1	18.5	15.5
Thermal efficiency	0.240	0.243	0.242	0.234	0.196
Waste gas temperature (°C)	491	481	480	482	480

Table 4.4d Power Generation Rates as A Function of Excess Air Ratio at
Biogas Volume Flow Rate 240L/min with 60% CH₄ [3]

Biogas supply at 240L/min					
Air flow (L/min)	1050	1100	1250	1400	1550
Excess air ratio	0.77	0.8	0.91	1.02	1.13
Power (kWe)	22.5	22.8	23.5	24.0	24.4
Thermal efficiency	0.261	0.265	0.273	0.279	0.283
Waste gas Temperature (°C)	517	513	506	506	506

Table 4.4e Power Generation Rates as A Function of Excess Air Ratio at
Biogas Volume Flow Rate 260L/min with 60% CH₄ [3]

Biogas supply at 260L/min					
Air flow (L/min)	1200	1250	1300	1400	1500
Excess air ratio	0.81	0.84	0.88	0.94	1.01
Power (kWe)	25.4	25.6	26.1	26.5	26.8
Thermal efficiency	0.272	0.275	0.280	0.284	0.287
Waste gas temperature (°C)	533	533	531	528	522

4.3 Effect of Inlet Gas Temperature

In this research, the waste heat is used to preheat the inlet gas (biogas and air), but not the water as done by Lin [3]. The results are shown in Figs. 4.11~16 and Table 4.5 a~c. The inlet gas are mixed in the heat exchanger and preheated to 80 and 120°C, while the inlet gas temperature without heating is around 40°C. The high pipe temperature of operating engine makes the inlet gas is heated to 40°C, even it does not pass through the heat exchanger. The volume of inlet gas expands with raised temperature, leading to a decrease in the aspiration ability of engine. At 120°C, the maximum allowable inlet gas volume starts to decrease from 1800L/min to about 1700L/min, leading to a

decrease of the maximum excess air ratio. For 180L/min biogas supply rate, it decreases from $\lambda=1.27$ to $\lambda=1.19$. For 160 L/min, it decreases from $\lambda=1.43$ to $\lambda= 1.34$. For 140 L/min, as mentioned before in sec.4.1, because the engine is about to shut down when the $\lambda > 1.58$, and the total amount of inlet gas is about 1700L/min. So the range of excess air ratio is not narrowed.

From Figs.4.11 and 4.12, for the biogas supply rate of 180L/min, the effect of inlet gas temperature on power generation and thermal efficiency is not obvious.

When the biogas supply rate decreases to 160L/min, the maximum excess air ratio reaches to 1.43. For this case, the effect of inlet gas temperature starts to appear when the excess air ratio is above 1.3 (see Figs. 4.13 and 4.14). When λ is greater than 1.3, the power generation and thermal efficiency increase with increasing inlet gas temperature. When the inlet gas temperature increases from 40°C to 80°C, the maximum power generation can increase from 16.1 to 17.4 kW, and the thermal efficiency can increase from 0.2306 to 0.2492.

When the biogas supply rate decreases to 140L/min, the maximum excess air ratio reaches to 1.58 (see Figs 4.15 and 4.16). When λ is greater than 1.3, the power generation and thermal efficiency increase with increasing temperature. The optimal λ , where the power and thermal efficiency start to drop, changes from $\lambda=1.20$ to $\lambda=1.39$. When the inlet gas is about 40°C without heating, the maximum power generation and thermal efficiency are 12.9 and 0.211 at $\lambda=1.2$. With 120 °C inlet gas, the corresponding highest power generation and thermal efficiency are 13.8 kW and 0.2259 at $\lambda=1.39$. Moreover, there is an obvious improvement at $\lambda=1.58$, the power generation

increases from 7.3 kW to 11.1 kW, and the thermal efficiency increases from 0.119 to 0.181.

Preheating the inlet gases makes the biogas and air mixing better. As the temperature rises, the collisions between gas molecules increase. The homogeneous mixture of fuel and air can make the combustor temperature become even during combustion process, so the engine performance becomes stable and better. However, the effect of increasing temperature starts to show up just when λ is around 1.3. From Figs.4.1 and 4.2, for 140L/min and 160L/min of biogas rate, the performance starts to decrease at $\lambda=1.2$ and $\lambda=1.29$, respectively. In such region, where the flame velocity is relatively low and the performance start to decrease, so the increasing temperature can play a significant role. Except this region, the flame velocity is relatively high, so the increasing temperature makes no effort on the engine performance.

The above results show that the improvement of preheat inlet gas is obvious when excess air ratio are relatively high (around $\lambda>1.3$), but the maximum excess air ratio is restricted by the inlet gas volume of engine. To solve this problem, turbocharging technology may be a suitable consideration. This technology uses waste gas of engine to drive compressor to increase the pressure of air entering the engine and to create more power.

Table 4.5a Power Generation Rates as A Function of Excess Air Ratio at
Biogas Supply Rate 140L/min and Inlet Gas Temperature 80~120°C

Biogas supply at 140L/min (73% CH ₄ , 80°C)									
Air flow (L/min)	780	870	970	1070	1170	1260	1360	1460	1540
Excess air ratio	0.8	0.89	0.99	1.09	1.20	1.29	1.39	1.5	1.58
Power (kWe)	7.8	10.6	11.2	12.2	12.8	13	13.3	13	9.8
Thermal Efficiency	0.127	0.173	0.183	0.199	0.209	0.212	0.217	0.212	0.160
Biogas supply at 140L/min (73% CH ₄ , 120°C)									
Air flow (L/min)	780	870	970	1070	1170	1260	1360	1460	1540
Excess air ratio	0.8	0.89	0.99	1.09	1.20	1.29	1.39	1.5	1.58
Power (kWe)	8	9.9	11.2	11.9	12.6	13.1	13.8	13.3	11.1
Thermal Efficiency	0.130	0.162	0.183	0.194	0.206	0.214	0.225	0.217	0.181

Table 4.5b Power Generation Rates as A Function of Excess Air Ratio at
Biogas Supply Rate 160L/min and Inlet Gas Temperature 80~120°C

Biogas supply at 160L/min (73% CH ₄ , 80°C)								
Air flow (L/min)	890	1000	1110	1220	1330	1440	1550	1600
Excess air ratio	0.8	0.89	0.99	1.09	1.19	1.29	1.39	1.43
Power (kWe)	9	13.2	14.8	15.3	15.8	16.5	17.3	17.4
Thermal Efficiency	0.128	0.189	0.211	0.219	0.226	0.236	0.247	0.249
Biogas supply at 160L/min (73% CH ₄ , 120°C)								
Air flow (L/min)	890	1000	1110	1220	1330	1440	1550	
Excess air ratio	0.8	0.89	0.99	1.09	1.19	1.29	1.39	
Power (kWe)	9	14	14.9	15.5	15.9	16.4	17.1	
Thermal Efficiency	0.128	0.200	0.213	0.222	0.227	0.234	0.244	

Table 4.5c Power Generation Rates as A Function of Excess Air Ratio at Biogas Supply Rate 180L/min and Inlet Gas temperature 80~120°C

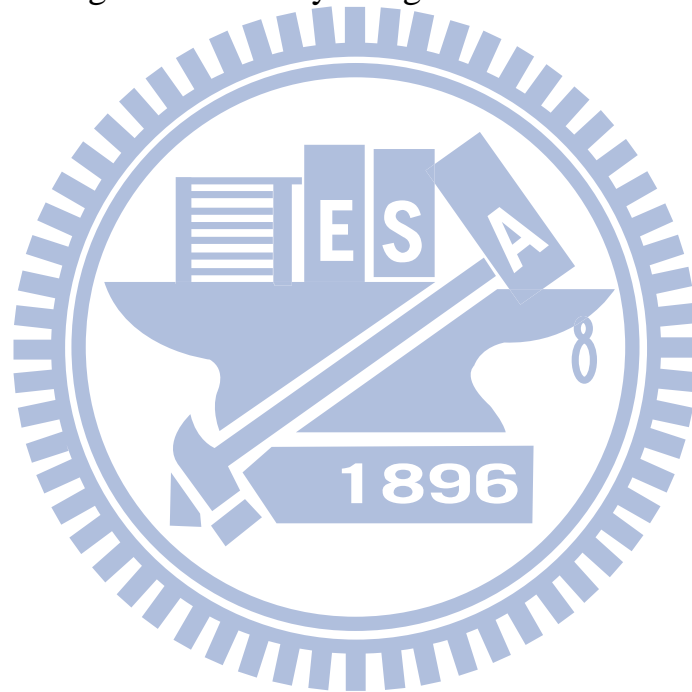
Biogas supply at 180L/min(73% CH ₄ ,80°C)						
Air flow(L/min)	1000	1120	1250	1370	1500	1600
Excess air ratio	0.79	0.89	0.99	1.09	1.19	1.27
Power (kWe)	10.7	16.2	16.9	18.2	19.1	19.5
Thermal Efficiency	0.136	0.206	0.215	0.231	0.243	0.248
Biogas supply at 180L/min(73% CH ₄ ,120°C)						
Air flow(L/min)	1000	1120	1250	1370	1500	
Excess air ratio	0.79	0.89	0.99	1.09	1.19	
Power (kWe)	10.9	15.9	17	18.8	19.7	
Thermal Efficiency	0.138	0.202	0.216	0.239	0.25	

4.4 Comparison with Other Researches

In this section, the comparisons with other experiments are made. In the research of Propatham et. al [11], they used a lime water scrubber to absorb carbon dioxide (CO₂) in biogas, carbon dioxide (CO₂) in biogas is reduced from 41% to 30%, then 20%. The highest corresponding thermal efficiencies are 0.262, 0.271 and 0.304 with methane concentration of 59%, 70% and 80%, respectively. Huang and Crookes [20] diluted natural gas by using CO₂ to simulate biogas as fuel in single-cylinder spark-ignition engine. The fraction of CO₂ in simulated biogas was ranged from 0 to about 40%, the maximum thermal efficiency is around 0.28. In this study, the corresponding maximum thermal efficiencies are 0.287 and 0.27 with methane concentration of 60% and 73%, respectively. The results reveal that the thermal efficiencies of above spark ignition engines are very close. However, they are lower than

commercial biogas engine, which thermal efficiency is about 30~40%. Therefore, the suggestions for improvement are given in the later chapter.

Ga et al. [18] used biogas-gasoline hybrid engine to test the conversion efficiency of the biogas. The results showed that 1 m³ of biogas can produce 1kW-h electricity. In their study, they didn't specifically point out the methane concentration of biogas. In this study, 1 m³ of biogas can produce about 1.9kW-h electricity. This improvement may result from that the methane concentration of biogas in this study is higher than the one of their study.



Chapter 5

Conclusions and Recommendations

5.1 Conclusions

This study is continuous effort of Lin's work [3], which carried out the electricity generation of the subproject 2 in a small swine farm in Miaoli. In Lin's research, 60% methane concentration of biogas was used. Later, the whole energy research program was moved to Taiwan Sugar swine farm in Taichung, whose size was about 1.5 times of that in Miaoli. The present experiments used 73% methane concentration of biogas. This study consisted three parts. Firstly, the effect of biogas supply rate together with different excess air ratio on generator performance was investigated. Secondly, a comparison with Lin's [3] results was made. Finally, a waste heat recovery system was applied to preheat the inlet gas (the mixture of biogas and air) under different temperatures and the preheating influence on the generator performance was analyzed.

According to the experiment results, this study can obtain the following conclusions:

1. At a given excess air ratio, the higher the biogas supply rate, the higher the power generation. With 73% CH₄ of biogas, the maximum power output is 26.7 kW at biogas supply of 260 L/min with $\lambda=0.84$. The maximum thermal efficiency and maximum CH₄ consumption ratio are 0.27 and 96.03% occurred at the biogas supply rate of 200 L/min with $\lambda= 1.1$. For the biogas supply rates above 180L/min, the power generation and thermal efficiency increase with the increase of excess air ratio.
2. With 73% CH₄ of biogas, when the biogas flow rate is 140L/min, it

provides a complete flammability domain between the upper and lower limits, which are $\lambda = 0.8$ and $\lambda = 1.58$, respectively.

3. When the methane concentration rises from 60% to 73%, the trends of power generation and thermal efficiency change, the corresponding lean misfire limit can be widened from $\lambda=1.13$ to $\lambda=1.27$ for 180L/min.
4. The power generation with 73% CH₄ of biogas are higher than the ones with 60% CH₄ of biogas, except the region around $\lambda<0.85$. However, the thermal efficiency increases with the increasing methane concentration just in the region of $\lambda>0.95$. For the mixture on the relatively rich side ($\lambda<0.95$), there is no benefit.
5. The effect of increasing inlet gas temperature on power generation and thermal efficiency is obvious when excess air ratios are relatively high ($\lambda>1.3$).
6. When the inlet gas temperature increases from 40°C to 120°C, for biogas supply rate of 140 L/min with $\lambda=1.58$. There is an obvious improvement, the power generation increases from 7.3 kW to 11.1 kW, and the thermal efficiency increases from 0.119 to 0.181.

5.2 Recommendations

Based on this study, the recommendations to solve the problems of the limit excess air ratio at high biogas supply rate and the future works are suggested:

1. Build dehumidifying system to reduce humidity of biogas.
2. Construct turbocharger to increase the pressure of air entering the engine.
3. Consider to use turbo engine instead of IC engine.

References

- [1] Falin Chen, Shyi-Min Lu , Eric Wang, Kuo-Tung Tseng, “Renewable energy in Taiwan”, *Renewable and Sustainable Energy Reviews*,14 ,2029–2038,2010
- [2] S. Rasi_, A. Veijanen, J. Rintala, “Trace compounds of biogas from different biogas production plants”, *Energy*,32,pp. 1375–1380 ,2007
- [3] Wei-Tsung Lin, “A Research for Electricity Generation by Using Biogas from Swine Manure for a Farm Power Requirement”, June 2010
- [4] Wen-Tien Tsai, Che-I Lin, “Overview analysis of bioenergy from livestock manure management in Taiwan”, *Renewable and Sustainable Energy Reviews*, 13, pp. 2682-2688, 2009.
- [5] Jung-Jeng Su, Bee-Yang Liu, Yuan-Chie Chang, “Emission of greenhouse gas from livestock waste and wastewater treatment in Taiwan”, *Agriculture Ecosystems and Environment*, 95, pp. 253-263, 2003.
- [6] Shang-Shyng Yang, Chung-Ming Liu, Yen-Lan Liu, “Estimation of methane and nitrous oxide emission from animal production sector in Taiwan during 1990–2000”, *Chemosphere*, 52, pp. 1381-1388, 2003.
- [7] Suiful Bari, “Effect of carbon dioxide on the performance of biogas/diesel dual-fuel engine”,WREC,1996
- [8] Phan Minh Duc , Kanit Wattanavichien, “Study on biogas premixed charge diesel dual fuelled engine”, *Energy Conversion and Management*, 48, pp. 2286 – 2308,2007
- [9] N. Tippayawong, A. Promwungkwa, P. Rerkkriangkrai, “Long-term operation of a small biogas/diesel dual-fuel engine for on-farm electricity

- generation”, *Biosystems Engineering*, 98, pp. 26-32, 2007.
- [10] F. N. Alasfour, “Nox emission from a spark ignition engine using 30% iso-butanol–gasoline blend: part 1–preheating inlet air”, *Applied Thermal Engineering*, 18, pp. 245–256, 1998
- [11] E. Porpatham, A. Ramesh , B. Nagalingam, “Investigation on the effect of concentration of methane in biogas when used as a fuel for a spark ignition engine”, *Fuel*, 87, pp.1651–1659, 2008
- [12] Pal Borjesson, Maria Berglund, “Environmental systems analysis of biogas systems—Part I: Fuel-cycle emissions”, *Biomass and Bioenergy*, 30, pp. 469-485, 2006.
- [13] G.H. Abd-Alia, H.A. Soliman, O.A. Badr, M.F. Abd-Rabbo, “Effect of diluents admissions and intake air temperature in exhaust gas recirculation on the emissions of an indirect injection dual engine”, *Energy Conversion and Management*, 42, pp.1033-1045, 2001
- [14] Konstantinos P. Tsagarakis, “Optimal number of energy generators for biogas utilization in wastewater treatment facility”, *Energy Conversion and Management*, 48 ,pp. 2694 – 2698, 2007
- [15] Semin, Abdul Rahim Ismail, Rosli Abu Bakar, “Effect of Diesel Engine Converted to Sequential Port Injection Compressed Natural Gas Engine on the Cylinder Pressure vs Crank Angle in Variation Engine Speeds”, *American J. of Engineering and Applied Sciences* 2 (1):154-159, 2009.
- [16] A.J. Torregrosa , P. Olmeda, J. Martin, B. Degraeuwe, “Experiments on the influence of inlet charge and coolant temperature on performance and emissions of a DI Diesel engine”, *Experimental Thermal and Fluid Science*,

- 30, pp. 633-641, 2006.
- [17] Paola Helena Barros Zarante , Jose Ricardo Sodre, “Evaluating carbon emissions reduction by use of natural gas as engine fuel”, *Journal of Natural Gas Science and Engineering*,1, pp. 216-220, 2009
- [18] Bui Van Ga-Le Minh Tien, Truong Le Bich Tram,Tran Hau Luong, “Biogas-Gasoline hybrid Engine” , Da Nang University,2008
- [19] Haeng Muk Cho,Bang-Quan He,“Spark ignition natural gas engines—A review”,48,pp.608-618,2007
- [20]Jindang Huang, R.J.Crookes, “Assessment of simulated biogas as a fuel for the spark ignition engine”,77,pp.1793-1801,1998
- [21] S. Swami Nathan, J.M. Mallikarjuna, A. Ramesh, “Effects of charge temperature and exhaust gas re-circulation on combustion and emission characteristics of an acetylene fuelled HCCI engine”,89,pp.515-521,2010
- [22] O. Badr, N. Alsayed and M. Manaf,“A parametric study on the lean misfiring and knocking limits of gas-fueled spark ignition engines”,18,pp.579-594,1998
- [23] G.Sridhar, P.J. Pual, H.S. Mukunda, “Biomass derived producer gas as a reciprocating engine fuel – an experimental analysis”,21,pp.61-72,2001
- [24] C.Tricase, M, Lombardi, “State of the art and prospects of Italian biogas production from animal sewage: Technical-economic considerations”,34,pp.477-485,2009
- [25] Chung, Y.C., K.L. Ho, C.P. Tseng, “ Two-stage biofilter for effective NH₃ removal from waste gases containing high

concentrations of H₂S”, J. Air Waste Manag. Assoc. 57:
337-347,2007

[26]Development of Rene wable Energy Sources in Germany 2009,
Federal Ministry for the Environment, Nature Conservation and
Nuclear Safty, 2009

[27]Arthur H. Lefebvre, “Gas Turbine Combustion”, Hemisphere
publishing corporation, 1983



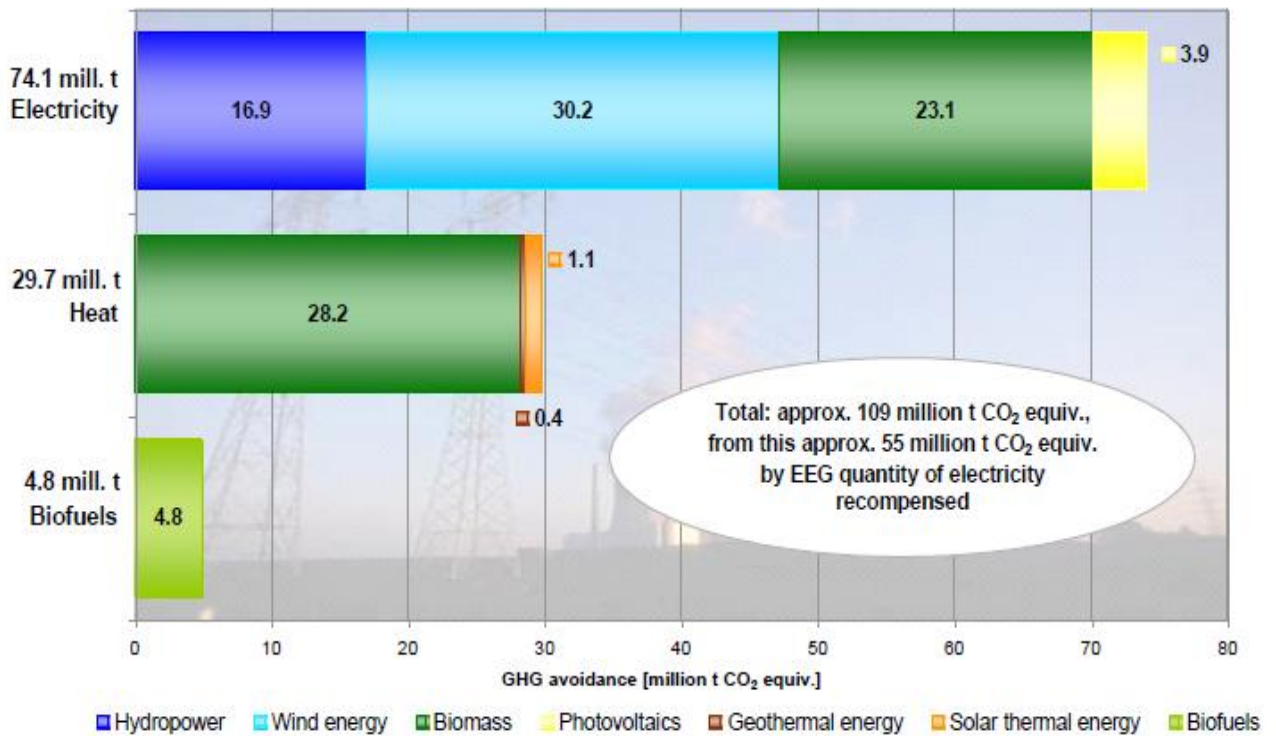


Fig. 1.1 Carbon Dioxide Emissions Avoided via the Use of Renewable Energy Sources in Germany 2009. [26]

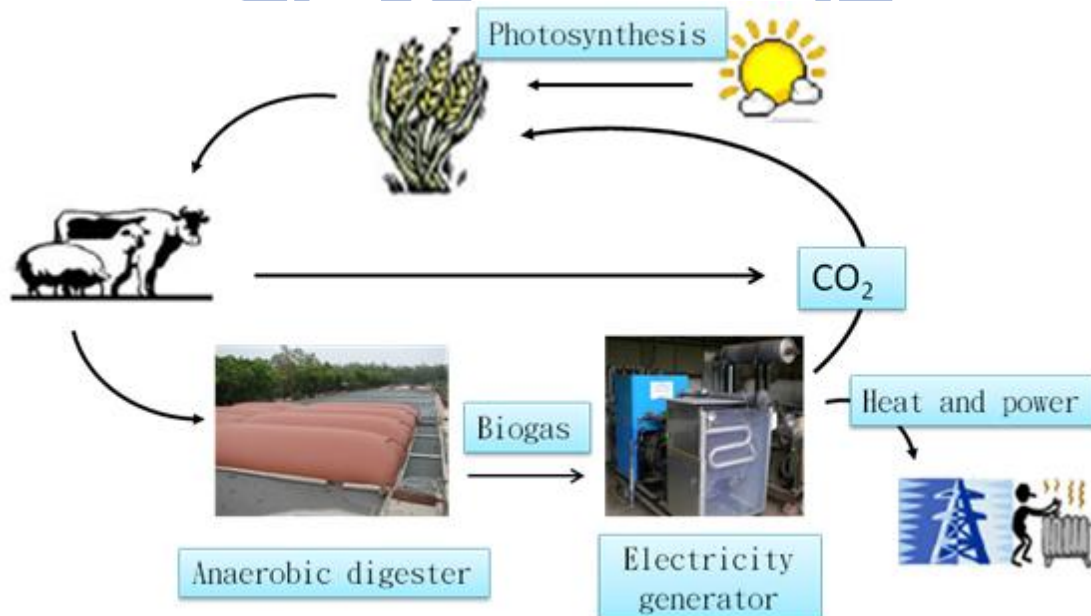


Fig. 1.2 Simple Carbon Cycle for Biogas [3]

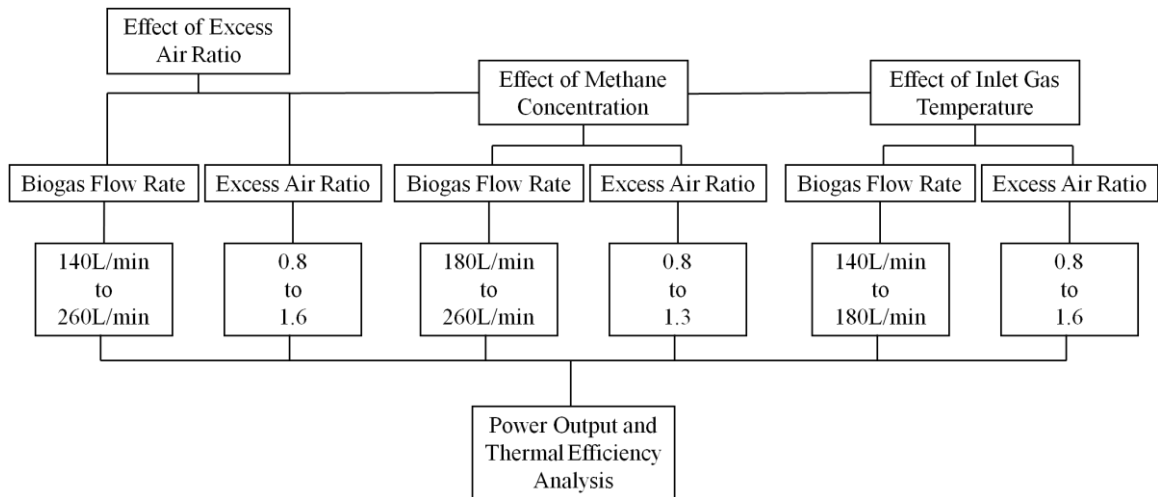
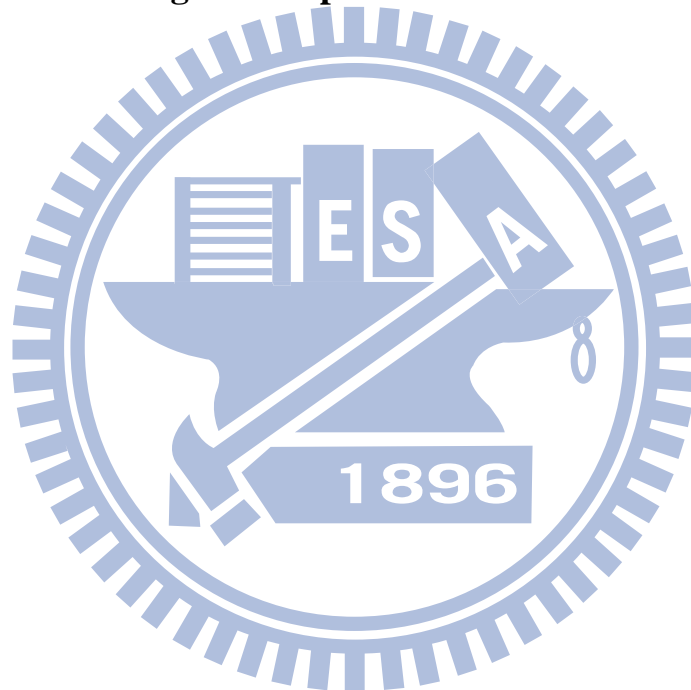


Fig. 1.3 Scope of this Research



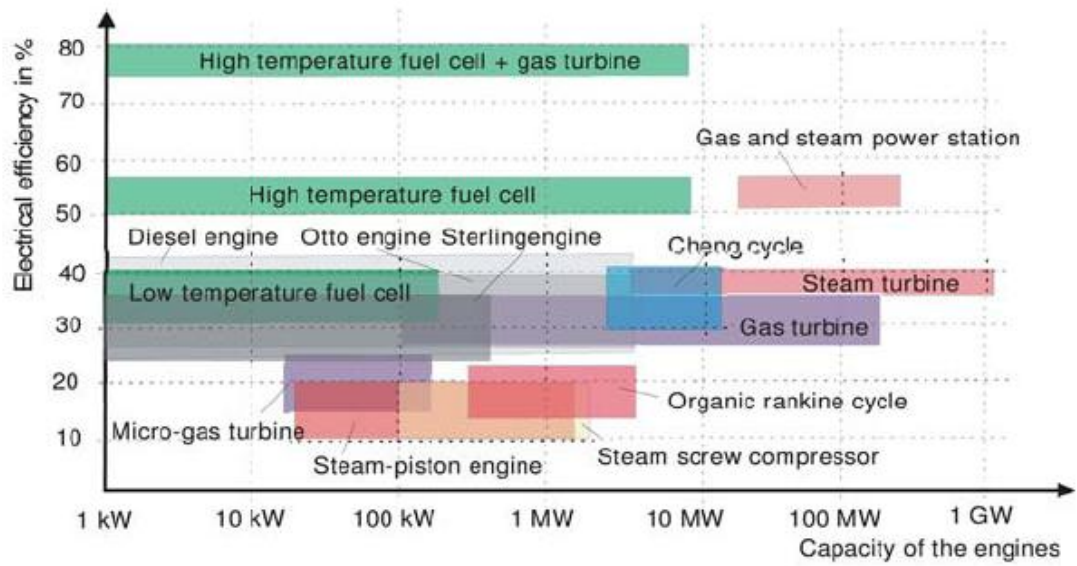
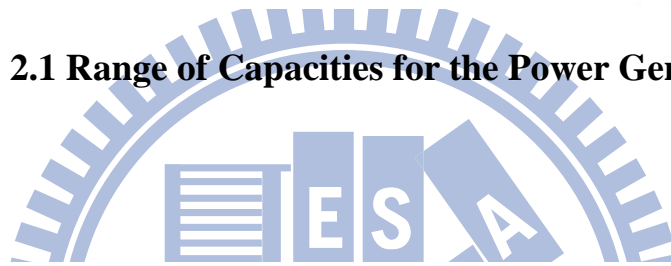


Fig. 2.1 Range of Capacities for the Power Generators



Feature	Four-stroke engine	Gas-Diesel engine	Stirling engine	Fuel cell	Gas turbine	Micro gas turbine
Capacity (kW)	<100	>150	<150	1-10000		30-110
Electrical efficiency	30-40%	35-40%	30-40%	40-70%	25-35%	15-33%
Pressure ratio	10:1	20:1	5:1	n.a.	5:1	5:1
Lifetime	Medium	Medium	Long	Very short	Long	Long
Alternative fuel in case of shortage of biogas	Liquid gas (gasoline)	Liquid gas	Any	Natural gas	Natural gas	Nature gas, fuel oil

Fig. 2.2 Values of Power Generators

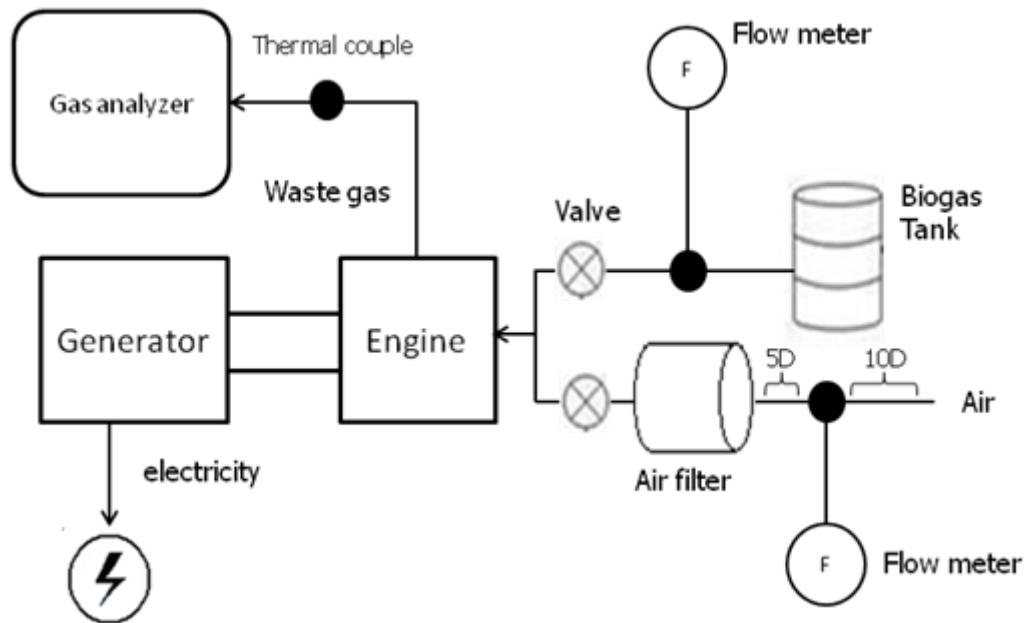


Fig. 3.1a Experiment Layout

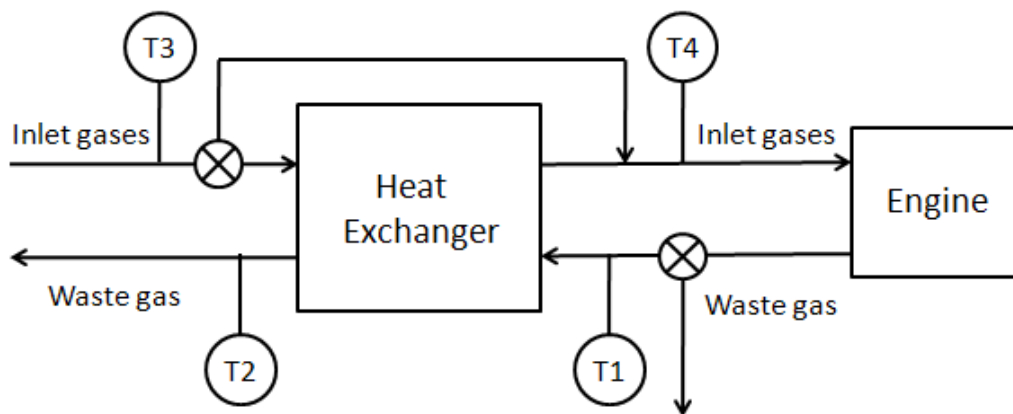
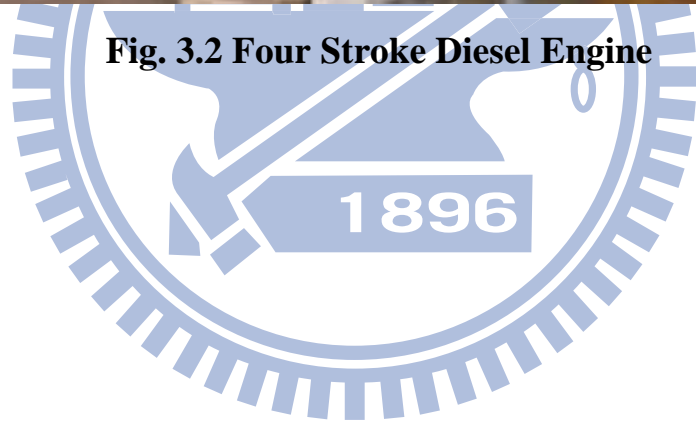


Fig. 3.1b Waste Heat Recovery Layout



Fig. 3.2 Four Stroke Diesel Engine



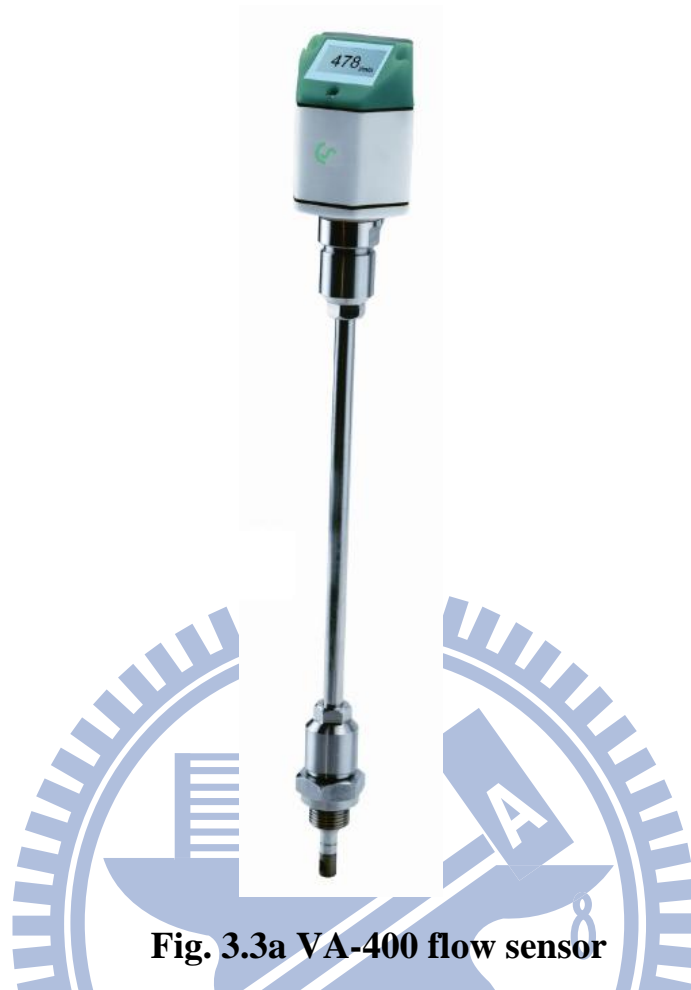


Fig. 3.3a VA-400 flow sensor

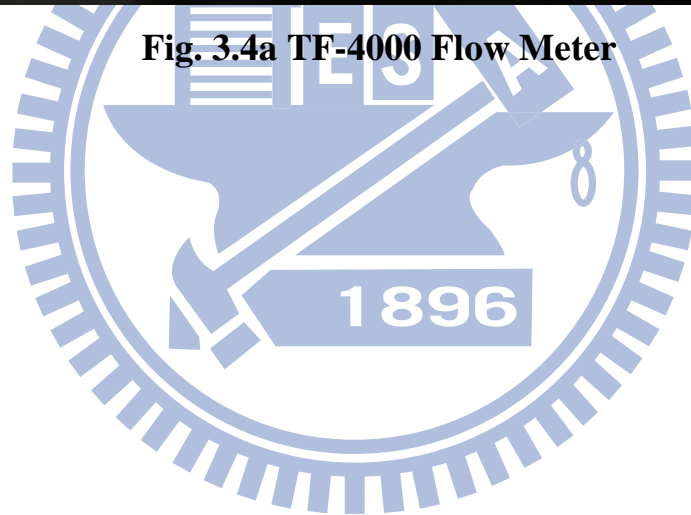
Technical data VA 400

Measured unit	m ³ /h, m ³ /min, l/min, cfm
Accuracy	± (3% of measured value + 0.3% full scale)
Medium	Air, gas, non explosive
Operating temperature	-30 ~ 140 °C probe tube -30 ~ 70 °C casing
Operating pressure	Up to 50 bar
Analogue output	Signal: 4 ~ 20 mA Scaling: 0 ~ max range
Pulse output	1 pulse per m ³
Power supply	12 ~ 30 VDC, 100 mA

Fig. 3.3b VA-400 Flow Sensor Data



Fig. 3.4a TF-4000 Flow Meter



Measuring Object		Air, N ₂ , & O ₂
Flow range		Min. 0 to 2L/min (nor)
		Max. 0 to 1000L/min (nor)
Gas pressure		0.1 to 1.0MPa
Accuracy		±2% F.S. (±1digit of indication accuracy added)
Response		Within 0.5 sec. (90% response)
Temp. & press. effect		0.1%F.S./°C · 0.1%F.S./0.1MPa
Rangiability		20:1 (Low flow cutoff: 5%F.S.)
Material of gas contact part	Main body	SCS14
	Sensor	SUS316, glass, platinum-iridium, & CTFE
	Seal	Fluororubber
Case		ABS resin (Non-waterproof)
Process connection		Rc1/4, Rc3/8, Rc1/2, & Rc3/4 (Depending on Model)
Electric connection		Exclusive cable with connector (1m long)
Installation posture		Horizontal or vertical direction
Indication		7 segments Red LED, 5 digits flow rate, totalization, setting value, & error
Indication value		Momentary flow rate: 0.00 to 99999. <ul style="list-style-type: none"> • A decimal point is displayed by automatic change. • An integrated value is not held at the time of a nonpower supply. Red LED × 2 pcs. Lighting when alarm is operating.. • Alarm value can be set by button switch.
Output	Aanalog	DC 0 to 5V (Output impedance: less than 50Ω), or DC 4 to 20mA (Load resistance: less than 600Ω @ 24V Power supply)
	Digital	RS-485 (Two-wire system, half-duplex communication) Baud rate: 2400, 4800 & 9600bps (Selection) Protocol: 8N1, ID address: 00 to 99
	Integrating pulse	Open collector (DC 24V, less than 10mA) • 0.2 to 10.0% F.S.-min/pulse (Possible to set up)
	Alarm	Open collector(DC24V, less than 100mA)
Power supply (Supplied by customer)		DC12 to 24V, max.210mA
CE marking		Acquired

Fig. 3.4b TF-4000 Flow Meter Data

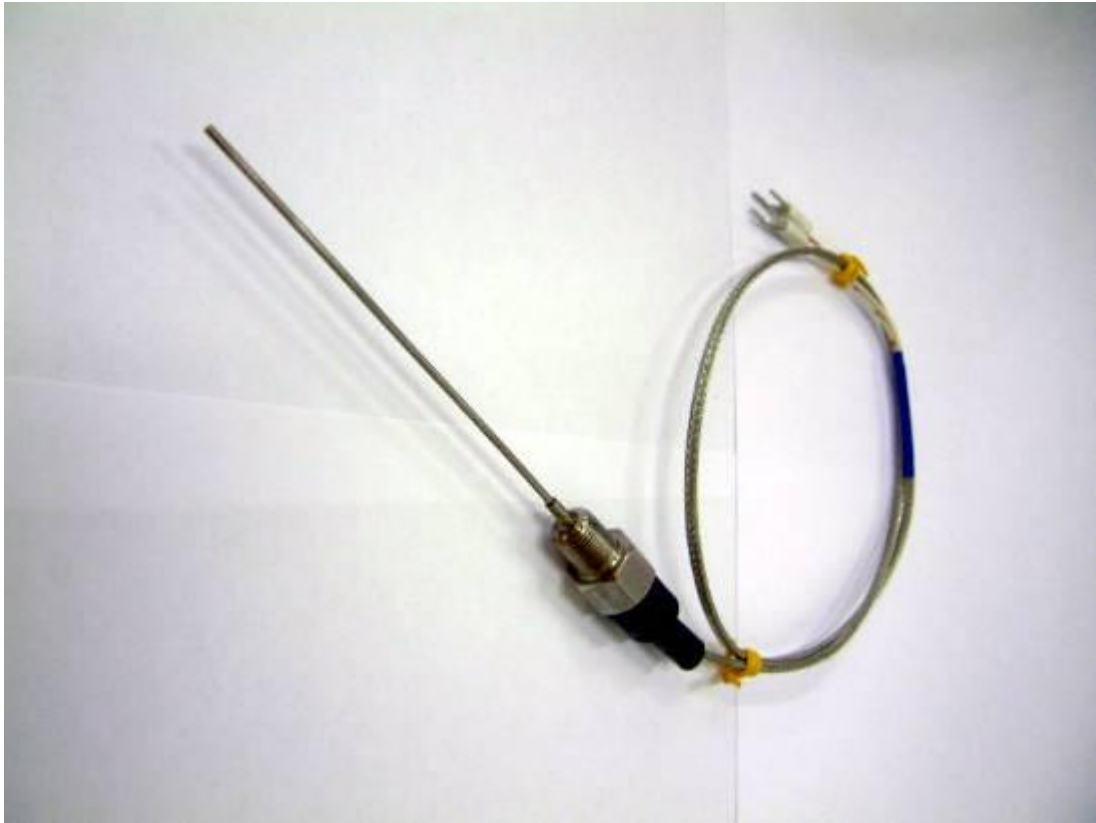


Fig. 3.5 K-Type Thermocouple



Fig. 3.6 HM5000 Gas Analyzer

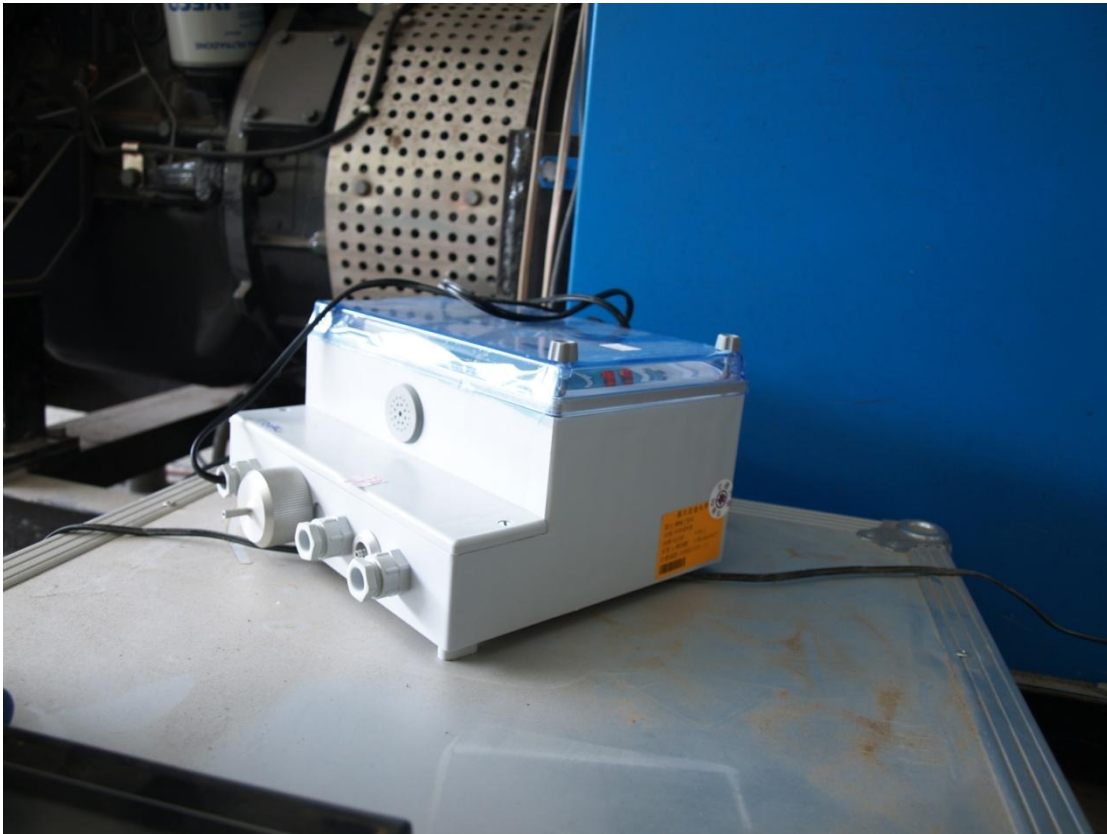


Fig.3.7 Guardian Plus Infra-Red Gas Monitor



Fig 3.8 Heat Exchanger



Fig. 3.9a CompactDAQ Chassis



Fig. 3.9b NI 9203 Analog Input Module



Fig. 3.9c NI 9211 Analog Input Module



Fig.3.10 Temperature Monitor



Fig.3.11 Center 311 Humidity Temperature Meter

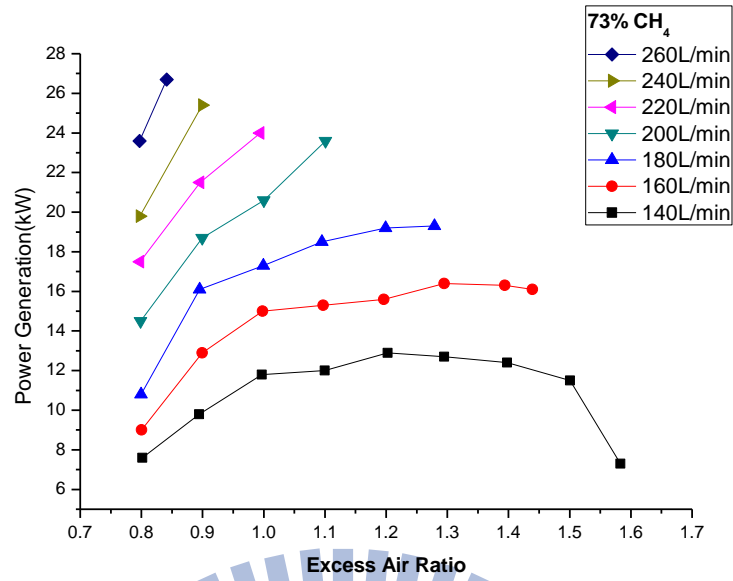


Fig. 4.1 Power generation v.s. excess air ratio at different biogas supply rates

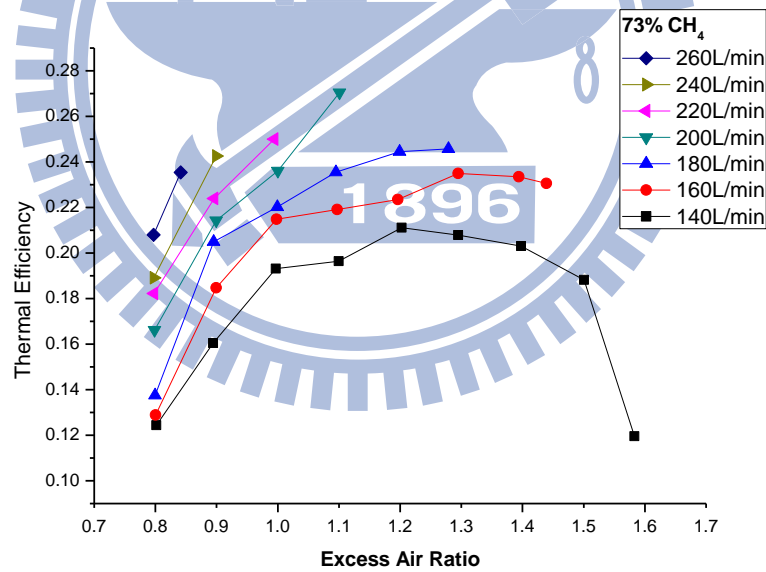


Fig. 4.2 Thermal efficiency v.s. excess air ratio at different biogas supply rates

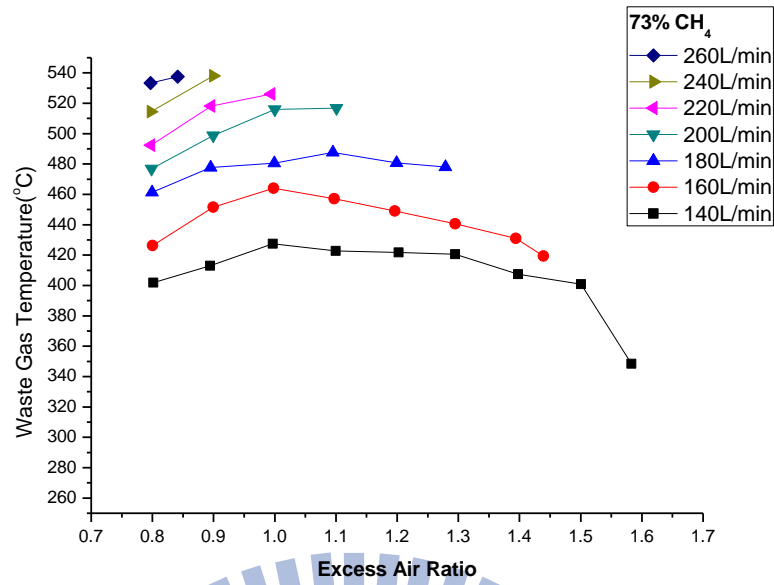


Fig. 4.3 Waste gas temperature v.s. excess air ratio with different biogas supply rates

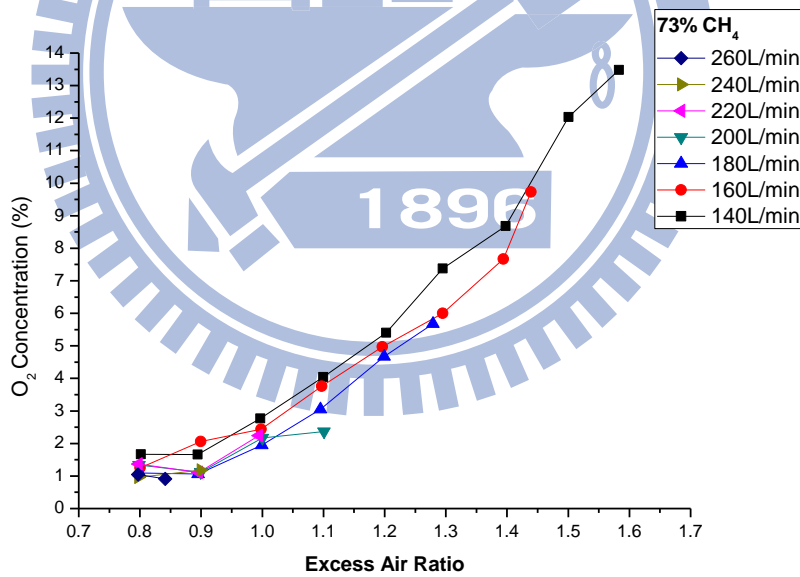


Fig. 4.4 O₂ concentration in waste gas v.s. excess air ratio with different biogas supply rates

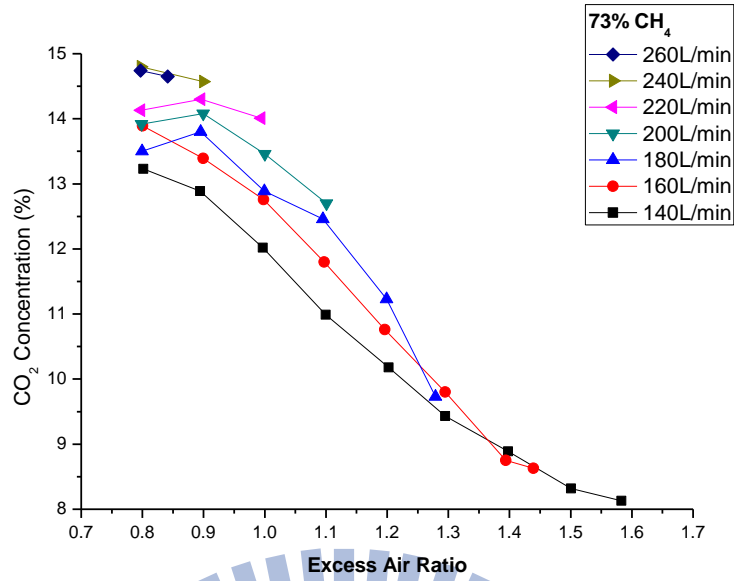


Fig. 4.5 CO₂ concentration in waste gas v.s. excess air ratio with different biogas supply rates

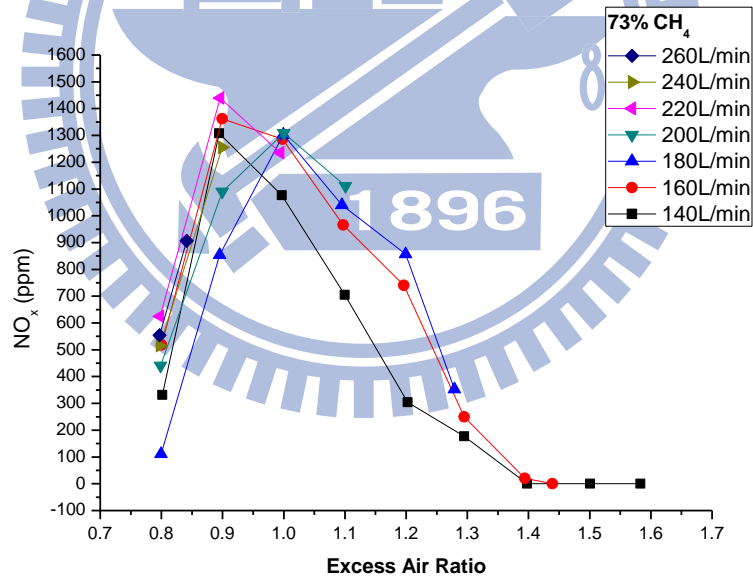


Fig. 4.6 NO_x concentration in waste gas v.s. excess air ratio with different biogas supply rates

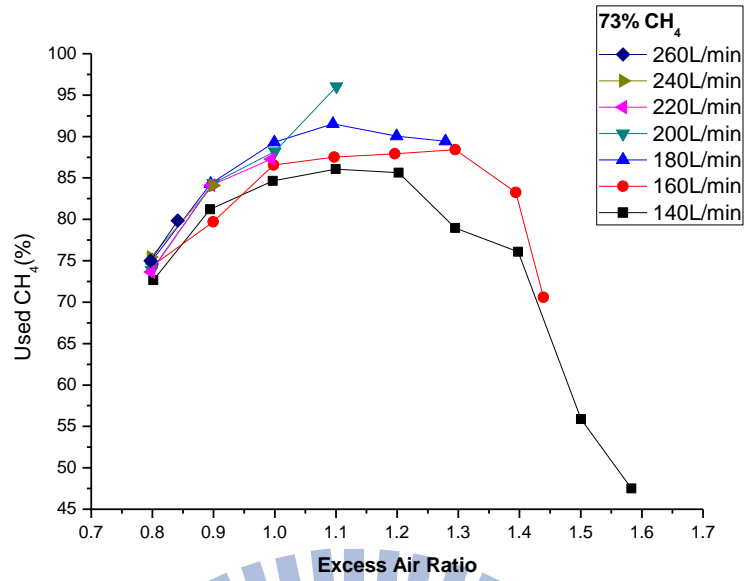


Fig. 4.7 Estimated CH₄ consumption ratios in combustion v.s. excess air ratio with different biogas supply rates

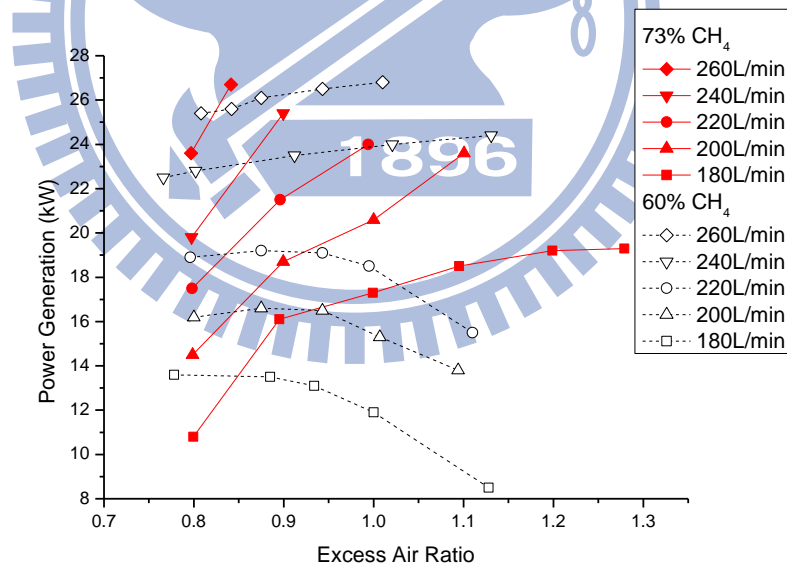


Fig. 4.8 Power generation with different methane concentrations of biogas

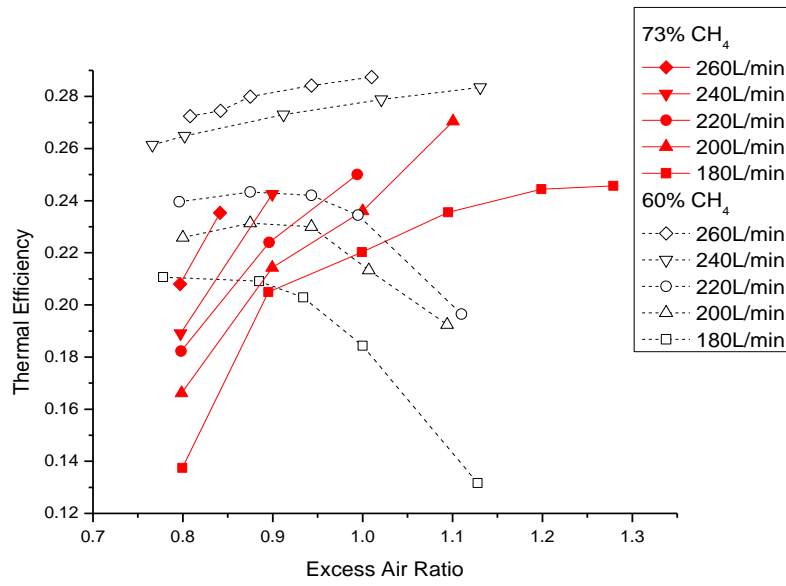


Fig. 4.9 Thermal efficiency with different methane concentrations of

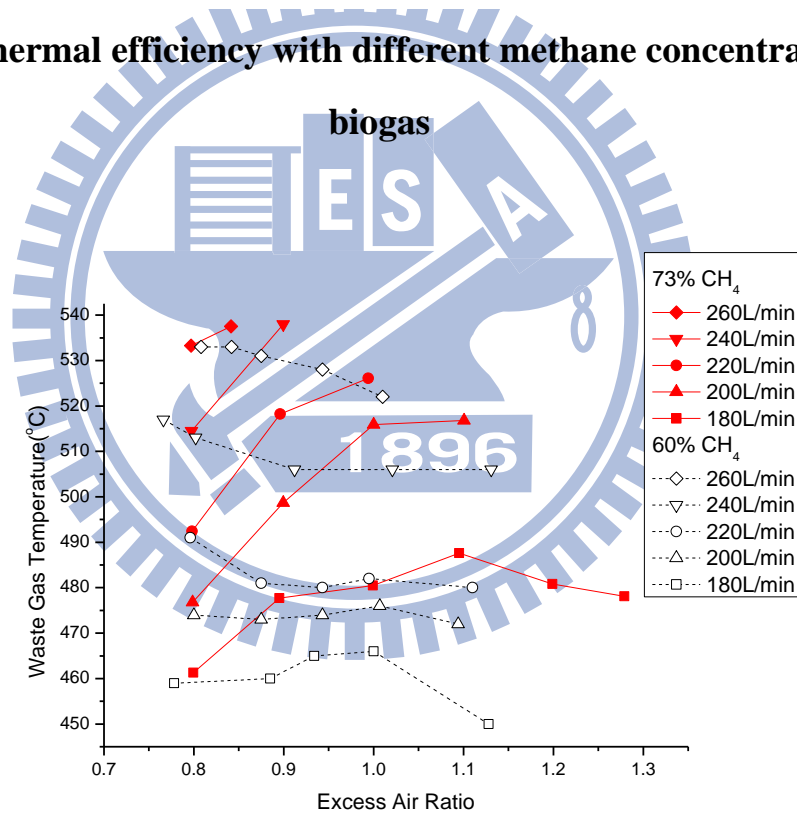


Fig. 4.10 Waste gas temperature with different methane concentrations of
biogas

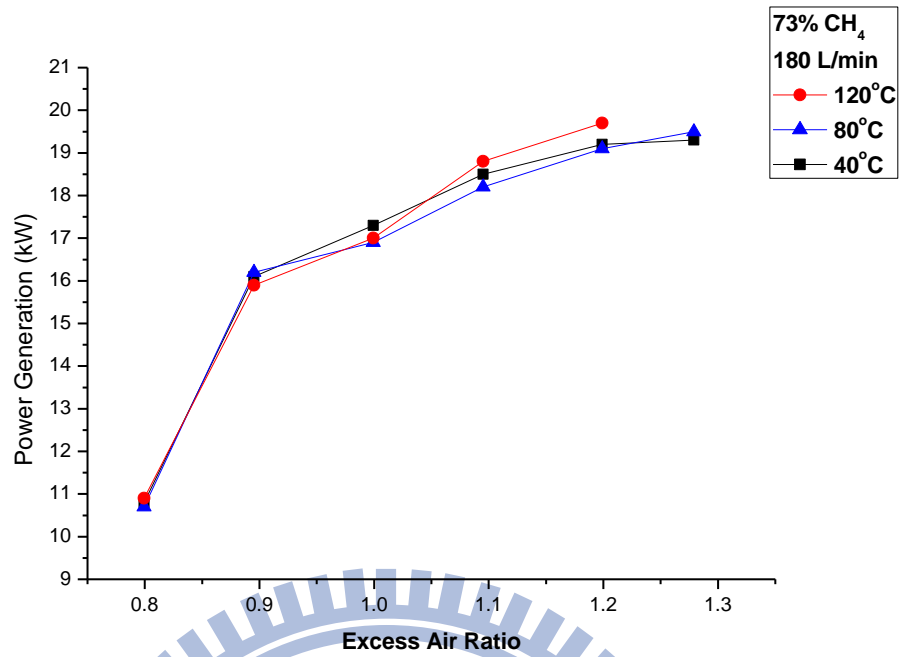


Fig. 4.11 Power generation of biogas supply rate 180 L/min v.s. excess air ratio with different inlet gas temperatures

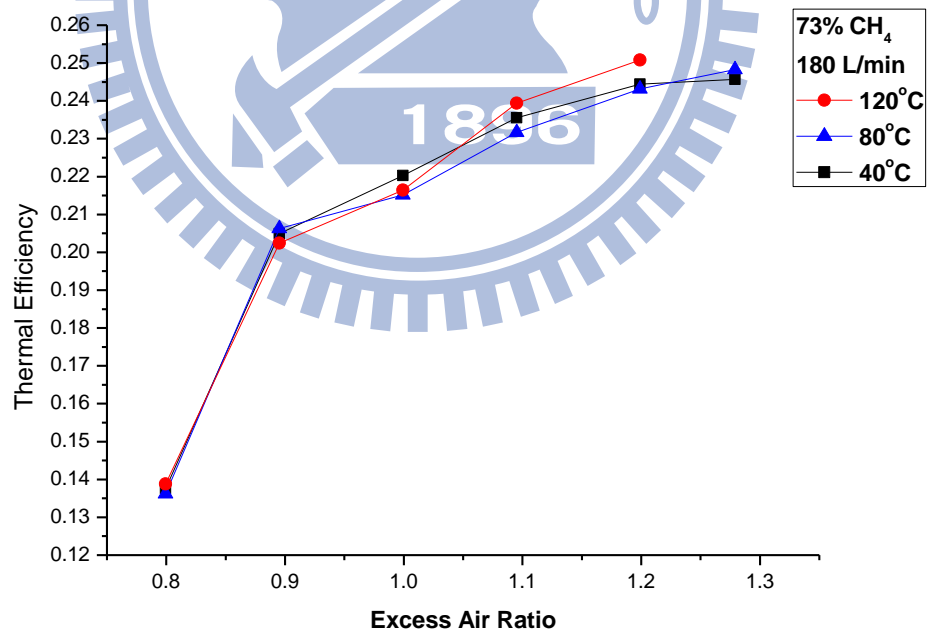


Fig. 4.12 Thermal efficiency of biogas supply rate 180 L/min v.s. excess air ratio with different inlet gas temperatures

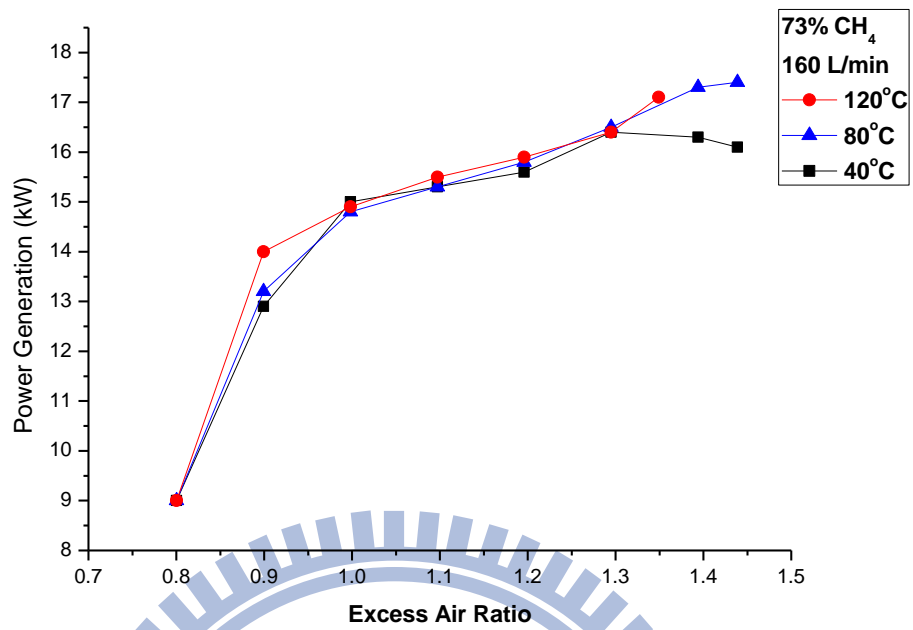


Fig. 4.13 Power generation of biogas supply rate 160 L/min v.s. excess air ratio with different inlet gas temperatures

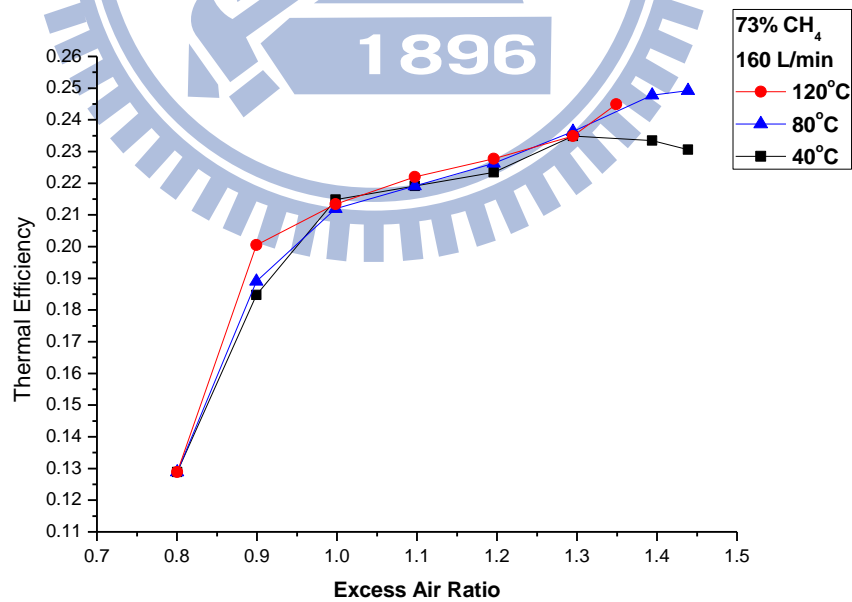


Fig. 4.14 Thermal efficiency of biogas supply rate 160 L/min v.s. excess air ratio with different inlet gas temperatures

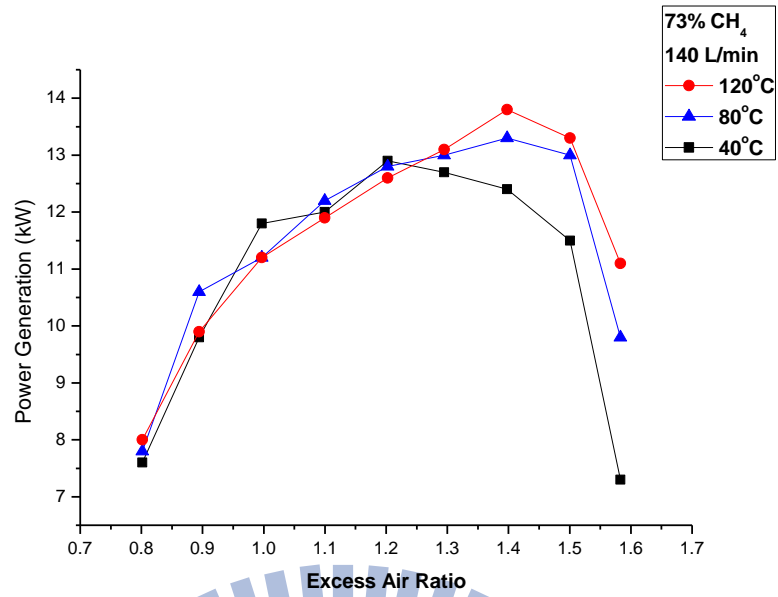


Fig. 4.15 Power generation of biogas supply rate 140 L/min v.s. excess air ratio with different inlet gas temperatures

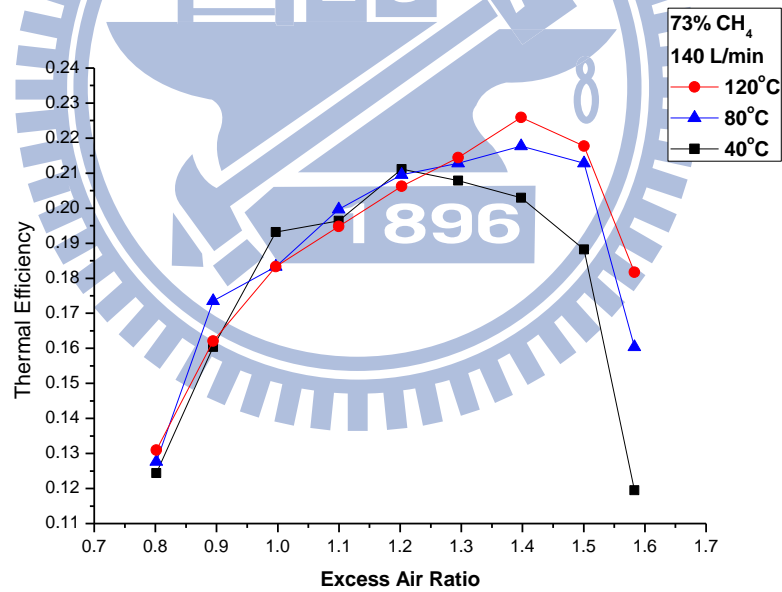


Fig. 4.16 Thermal efficiency of biogas supply rate 140 L/min v.s. excess air ratio with different inlet gas temperatures